



รายงานวิจัยฉบับสมบูรณ์

โครงการ การศึกษาปฏิกิริยาเอทธิลีนอีพอกซิเดชันในระบบประกายไฟฟ้าพลาสมา

โดย ผศ.ดร.ฐิติพร สุทธิกุล และคณะ

รายงานวิจัยฉบับสมบูรณ์

โครงการ การศึกษาปฏิกิริยาเอทธิลีนอีพอกซิเดชันในระบบประกายไฟฟ้าพลาสมา

ผู้วิจัย สังกัด

- 1. ผู้ช่วยศาสตราจารย์ ดร.ฐิติพร สุทธิกุล มหาวิทยาลัยเทคโนโลยีพระจอมเกล้าพระนครเหนือ
- 2. ศาสตราจารย์ ดร. สุเมธ ชวเดช วิทยาลัยปิโตรเลียมและปิโตรเคมี จุฬาลงกรณ์มหาวิทยาลัย

สนับสนุนโดยสำนักงานคณะกรรมการการอุดมศึกษาและสำนักงานกองทุนสนับสนุนการวิจัย

(ความเห็นในรายงานนี้เป็นของผู้วิจัย สกอ. และ สกว. ไม่จำเป็นต้องเห็นด้วยเสมอไป)

บทคัดย่อ

รหัสโครงการ: MRG5980154

ชื่อโครงการ: การศึกษาปฏิกิริยาเอทธิลีนอีพอกซิเดชันในระบบประกายไฟฟ้าพลาสมา

ชื่อนักวิจัย และสถาบัน: ผศ.ดร.ฐิติพร สุทธิกุล มหาวิทยาลัยเทคโนโลยีพระจอมเกล้าพระนครเหนือ

อีเมล์: thitiporn2528@hotmail.com, thitiporn.su@kmutnb.ac.th

ระยะเวลาโครงการ: 2 ปี

บทคัดย่อ:

ในงานวิจัยนี้เป็นการศึกษาปฏิกิริยาอีพอกซิเดชั่นในระบบพลาสมาอุณหภูมิต่ำชนิดใด-อิเล็คทริคแบริเออร์ดิสซาร์จ(ดีบีดี)แบบทรงสี่เหลี่ยมด้านขนาน โดยใช้กระจกขรุขระสองแผ่นเป็น ฉนวน ภายใต้สภาวะอุณหภูมิห้องและความดันบรรยากาศ การป้อนแยกของก๊าซเอธีลีนกับ ออกซิเจนถูกใช้ในการทดลองเพื่อเพิ่มประสิทธิภาพของปฏิกิริยาอีพอกซิเดชั่นและลดการเกิด ปฏิกิริยาข้างเคียง จากการศึกษาผลกระทบของความต่างศักย์ไฟฟ้า ความถี่ไฟฟ้า อัตราส่วน โดยโมลของออกซิเจนต่อเอธีลีน และ ตำแหน่งในการป้อนเอธีลีน ที่มีต่อปฏิกิริยา พบว่า ระบบ พลาสมาที่ใช้ผลิตค่าการเลือกสรรในการเกิดเอธีลีนออกไซด์และผลได้ของเอธีลีนออกไซด์สูงสุด ที่ 68.15% และ 10.88% ตามลำดับ ภายใต้สภาวะดำเนินการที่เหมาะสม คือ 23 กิโลโวลต์ 500 เฮิรตซ์ อัตราส่วนโดยโมลของออกซิเจนต่อเอธีลีน 1:5 และ ตำแหน่งในการป้อนเอธีลีน 0.5 โดย ผลได้ของเอธีลีนออกไซด์มีค่าเป็นสองเท่าเมื่อเปรียบเทียบกับระบบพลาสมาแบบเดิมที่ใช้กระจก แผ่นเรียบทั้ง 1 และ 2 แผ่น

คำหลัก: ปฏิกิริยาอีพอกซิเดชั่น, เอธีลีนออกไซด์, ไดอิเล็คทริคแบริเออร์ดิสชาร์จ, ตำแหน่งใน การป้อนเอธีลีน Abstract

Project Code: MRG5980154

Project Title: Ethylene Epoxidation in Low-Temperature AC Dielectric Barrier

Discharge: Effects of Dielectric Surface Roughness, number of Dielectric Barrier, and

Oxygen Source

Investigator: Assist. Prof. Thitiporn Suttikul

King Mongkut's University of Technology North Bangkok

E-mail Address: thitiporn2528@hotmail.com, thitiporn.su@kmutnb.ac.th

Project Period: 2 years

single or two smooth dielectric glass plates.

Abstract:

The objective of this work was to investigate ethylene oxide (EO) performance in a low-temperature parallel plate dielectric barrier discharge (DBD) system with two frosted glass plates as the dielectric barrier material under ambient temperature and atmospheric pressure. A separate feed technique was used to reduce all undesirable reactions in order to maximize ethylene oxide production. The effects of applied voltage, input frequency, and O2/C2H4 feed molar ratio, as well as ethylene feed position, on ethylene epoxidation activity were examined. The DBD system with two frosted glass plates was found to provide the highest EO selectivity of 68.15% and the highest EO yield of 10.88% at 23 kV, 500 Hz, an O₂/C₂H₄ feed molar ratio of 1:5, and an ethylene feed position fraction of 0.5, which gave double the EO yield of both DBD systems with

Keywords: Epoxidation, Ethylene oxide, Dielectric barrier discharge, C₂H₄ feed

position

2

Executive summary

Introduction to the research problem and its significance

Since global economic and population growth lead to the expansion of many industries, the specific demand of petrochemical products is currently increasing. Ethylene oxide, epoxyethane, dimethylene oxide, oxacyclopropane, or oxirane (C₂H₄O, EO) is the one of important industrial chemicals that is used as a substrate to produce several useful chemicals.

For EO applications, it can easily be formed polyethylene glycol or polyethylene oxide, which is very useful in surfactant and cosmetic industries. In addition, ethylene glycol generated from EO is commonly used as an automotive coolant and antifreeze. The main advantage of ethylene glycol is the production of polyester polymers. Moreover, EO is used in many industries such as for foodstuffs and medical supplies, pharmaceuticals, textiles, and adhesives (Mendes et al., and Watkinson, 2007).

The important method to synthesize effectively commercial EO from ethylene is the gasphase partial oxidation of ethylene or ethylene epoxidation with using $Ag/(LSA)\Omega-Al_2O_3$ catalysts. Promoters such as Re, Cl, Au, Pd, Cu, and Cs were proved to enhance the EO selectivity (Campbell et al., 1986; Epling et al., 1997; Geenen et al., 1982; Goncharova et al., 1995; Jankowiak et al., 2005). Nonetheless, this commercial process can give higher EO selectivity; a high temperature operation is required to efficiently motivate the conventional catalytic processes. Therefore, finding a new method with using lower energy consumption and fewer problems from catalyst deactivation is of great interest.

Plasma techniques is a promising technique and it can be employed for various applications. Plasma can be divided into thermal and non-thermal plasma. Non-thermal plasma is one kind of electric gas discharges. The advantage of this non-thermal plasma over thermal plasma is the generated high energy electrons have an extremely high temperature (approximately 10⁴-10⁵ K), while the bulk gas has a relatively low temperature (close to ambient temperature) (Rosacha et al., 1993; Suhr et al., 1984). Therefore, it can be operated at ambient temperature and atmospheric pressure, leading to low energy consumption. Dielectric Barrier Discharge (DBD) is one type of nonthermal plasma and it was used in various applications because of its fairly uniform plasma distribution. For discharge generation, electrons receive sufficient energy from applied voltage to overwhelm the potential barrier of metallic electrode surface and then the generated electrons can directly collide with the gaseous substances that present in plasma zone to create new ions and neutral species. Moreover, the dissociated species or generated excited species are typically higher reactivity than neutral species at the ground state. The examples of chemical synthesis using the non-thermal plasma are oxidations of olefins and aromatics (Suhr et al., 1988; Patiño et al., 1996; Sreethawong et al., 2007). In addition, the using non-thermal plasma technique can provides several advantages over than the conventional catalytic process. One of them is operation at low temperature close to room temperatures and near or insignificantly higher than atmospheric

pressure. However, this method provides less EO selectivity than the catalysis technique (Pietruszka et al., 2004).

The DBD reactor generally consists of one or more dielectric layers between two electrodes. The configuration was reported to influence the efficiency of EO production and the cylindrical DBD provided superior ethylene epoxidation performance as compared to the parallel plate DBD (Sreethawong et al., 2010). The input power and reactor thickness significantly affected the performance of methane reforming (Rueangjitt et al., 2011), as corresponding to the study that the dielectric material and thickness remarkably changed the plasma behavior (Thomas et al., 2009).

For these reasons, ethylene epoxidation will be investigated in a low-temperature parallel dielectric barrier discharge (DBD) reactor by focusing on the effects of dielectric barrier surface of two types of smooth and rough surfaced glass plates. The effects of various operating parameters, including O_2/C_2H_4 feed molar ratio, applied voltage, input frequency, and ethylene feed position on the ethylene epoxidation activity in the parallel DBD systems with two rough-surfaced glasses will be examined for maximum EO production performance. In comparison, the DBD system with using a smooth-surfaced glass, a rough-surfaced glass, and two rough-surfaced glasses will be investigated under their optimum conditions in order to determine improvement of ethylene epoxidation activity. The effect of oxygen source will next be studied in the DBD system. Pure oxygen will be replaced with nitrous oxide (N_2O) or air for this reaction in order to comparatively study the effect of oxygen source.

Objectives

The overall objective of this study is to investigate the ethylene epoxidation in a low-temperature parallel plate DBD system in order to improve ethylene oxide production. The specific objectives of this study are:

- to investigate the ethylene epoxidation performance in a low-temperature parallel plate
 DBD system with two rough glass plates as a dielectric barrier
- 2) to comparatively investigate the effects of operational parameters, including ethylene feed position, O₂/C₂H₄ molar ratio, applied voltage, input frequency, and calcination temperatures on the activity of ethylene epoxidation.
- 3) to comparatively study the effects of dielectric surface roughness, by using smooth-surface and rough-surfaced glass plates, and number of dielectric barriers to investigate the effects of oxygen source on the epoxidation activity
- 4) to investigate oxidizing agents such as nitrous oxide (N₂O) and air compared to the pure oxygen (O₂), on the ethylene epoxidation performance

Methodology

1) Materials

Both smooth-surfaced and rough-surfaced glass plates will be cleaned with distilled water and acetone before being used as the dielectric barrier. The 99.995% helium (high purity

grade), 40% ethylene in helium (± 1% uncertainty), and 97% oxygen in helium (± 1% uncertainty) will be specially blended by Thai Industrial Gas Co., Ltd and used as a balancing gas and reactant gases, respectively. Whereas, the 30% ethylene oxide in helium (± 1% uncertainty) will be used as a standard gas to obtain the calibration curve of gas chromatography (GC) for EO analysis.

2) Dielectric Barrier Characterization

The X-ray fluorescence (XRF) will be widely used to measure the elemental composition of materials. The XRF patterns of both smooth-surfaced and rough-surfaced glass plates will be obtained by using a using PANalytical analysis instruments with AXIOS & SUPERQ version 4.0 systems. IQ+ program will be used to measure and to analyze the samples. A filed emission scanning electron microscope (FE-SEM, JEOL 5200-2AE) operated at 1 to 20 kV will be used to observe the surface morphology of all glass plates. The sample placed on the stub will be coated by platinum (Pt) prior to being loaded into the microscope. The atomic force microscope (AFM) will be employed to observe surface roughness of all glass plates. The AFM (XE-100 Series Park Systems SPM Controller) will be operated with non-contact mode, scan of 20 μm, and a scan rate of 0.1 Hz.

3) Experimental Setup and Reaction Activity Experiments

The experimental study of ethylene epoxidation will be investigated in a parallel dielectric barrier discharge (DBD) reactor at ambient temperature and atmospheric pressure. The schematic of experimental setup of using the DBD system is shown in Figure 1. The reactor configuration is shown in Figure 2. The reactor sizes are 1.5 cm height x 5.5 cm width x 17.5 cm length for inner dimension and 3.9 cm height x 9.5 cm width x 21.5 cm length for outer dimension, and distance between ethylene feed positions is 3.5 cm. Between the two electrodes, there is a dielectric glass plate. The gap distance between the two electrodes is fixed at 7 mm (Suttikul *et al.*, 2011).

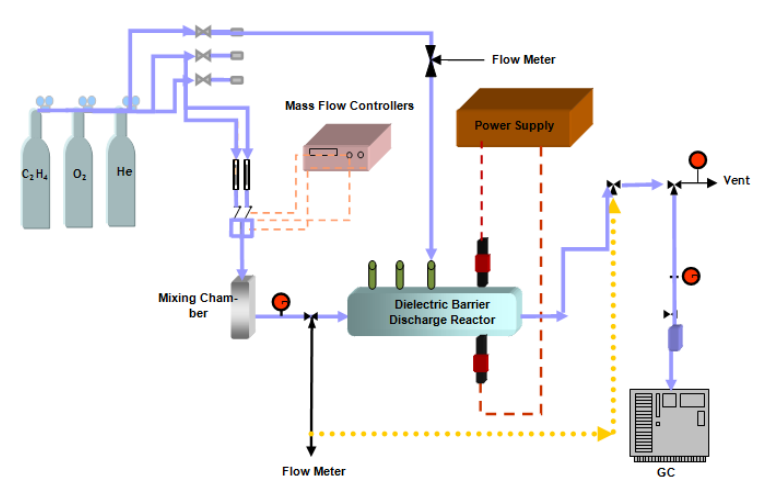


Figure 1 Schematics of experimental setup for ethylene epoxidation reaction using parallel DBD.

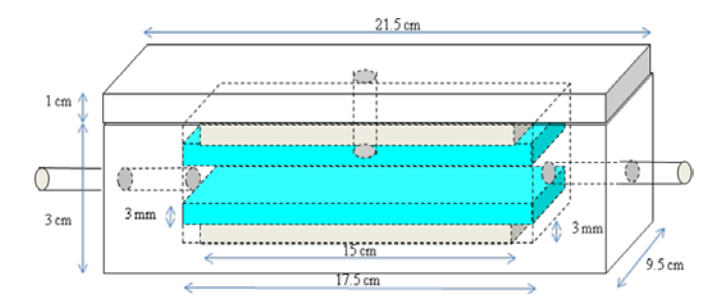


Figure 2 Parallel DBD reactor configurations.

The reactant gases (ethylene and oxygen, balanced with helium) flowing through the reactor will be controlled by a set of electronic mass flow controllers. All reactant lines have 7 μm in-line filters before passing through the mass flow controllers in order to trap any foreign particles. The reactor pressure will be controlled via a needle valve. The outlet of reactor will either be vented to the atmosphere via rubber tube exhaust or enter an on-line gas chromatograph (GC) to analyze the product gases. The moisture in the effluent gas will be removed by a water trap before entering to the on-line GC. The GC is equipped with both a thermal conductivity detector (TCD) and a flame ionization detector (FID). For the TCD channel, a packed column (Carboxen 1000) will be used for separating the product gases, which are hydrogen (H₂), oxygen (O₂), carbon monoxide (CO), carbon dioxide (CO₂), and ethylene (C₂H₄). For FID channel, a capillary column (OV-Plot U) will be used for the analysis of ethylene oxide (EO) and other by-product gases, i.e. CH₄, C₂H₂, C₂H₆, and C₃H₈. The composition of the product gas stream will be determined by the GC every 20 min. When the system reaches steady state, an analysis of the outlet gas compositions will be performed at least three times. The experimental data under steady state conditions will be averaged and then used to evaluate the performance of the plasma system.

To evaluate the system performance, the C_2H_4 and O_2 conversions and the selectivity for products, including EO, CO, CO_2 , H_2 , CH_4 , C_2H_2 , C_2H_6 , and traces of C_3 , will be considered. The conversion of both C_2H_4 and O_2 will be calculated from the following equation:

$$%Reactant conversion = \frac{(moles of reactant in - moles of reactant out) \times 100}{moles of reactant in}$$
(1)

$$\label{eq:product} \mbox{$^{\circ}$ Product selectivity} = \frac{\mbox{$[(number\ of\ carbon\ or\ hydrogen\ atom\ in\ product\)(moles\ of\ product\ produced\)]\times 100}{\mbox{$[(number\ of\ carbon\ or\ hydrogen\ atom\ in\ C2H4)(moles\ of\ C2H4\ converted\)]}}$$

%EO yield =
$$\frac{\text{(\% C2H4 conversion)} \times \text{(\% EO selectivity)}}{100}$$
 (3)

In addition, power consumption was calculated in a unit of Ws per C₂H₄ molecule converted or per EO molecule produced using the following equation:

Power consumption =
$$\frac{P \times 60}{N \times M}$$
 (4)

where P = Power(W)

N = Avogadro's number = 6.02×10^{23} molecules/mol

M = Rate of converted C_2H_4 molecules in feed or rate of produced EO molecules (mol/min).

Results and discussion

1) Surface Characterization Results

The chemical compositions of the clear and frosted glass plates are shown in Table 1. The compositions of both glass plates were almost the same with a major content of silica oxide (SiO_2) of more than 70%. As shown in Fig. 3, the roughness of the frosted glass plate used in this study is in the range of 0.18-1.22 μ m, as measured by AFM. In addition, the AFM and SEM results indicate that the surface morphology of the frosted glass plate were heterogeneous (see Fig. 3 and 4).

Table 1 Chemical compositions of clear and frosted glass plates analyzed by XPF

Chemical compositions	Clear glass plate (wt.%)	Frosted glass plate (wt.%)
SiO ₂	71.1	74.3
Na ₂ O	13.5	9.5
CaO	10.9	11.9
MgO	2.9	2.7
Al_2O_3	1.0	1.1
Other	0.6	0.5

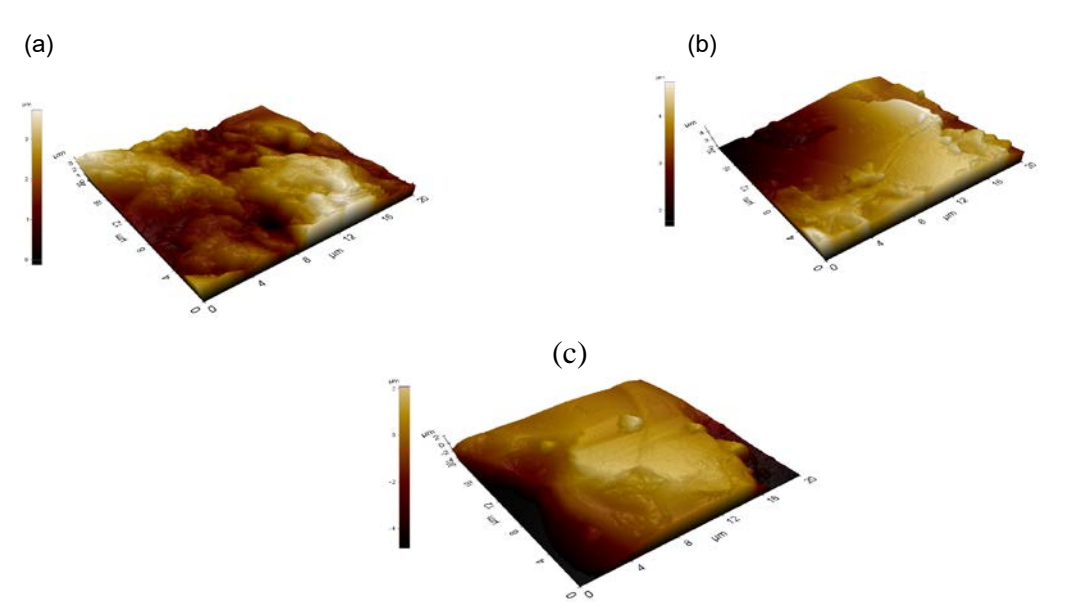


Figure 3 Surface images of the frosted glass plate by AFM (a) left-edge side, (b) middle-edge side, and (c) right-edge side

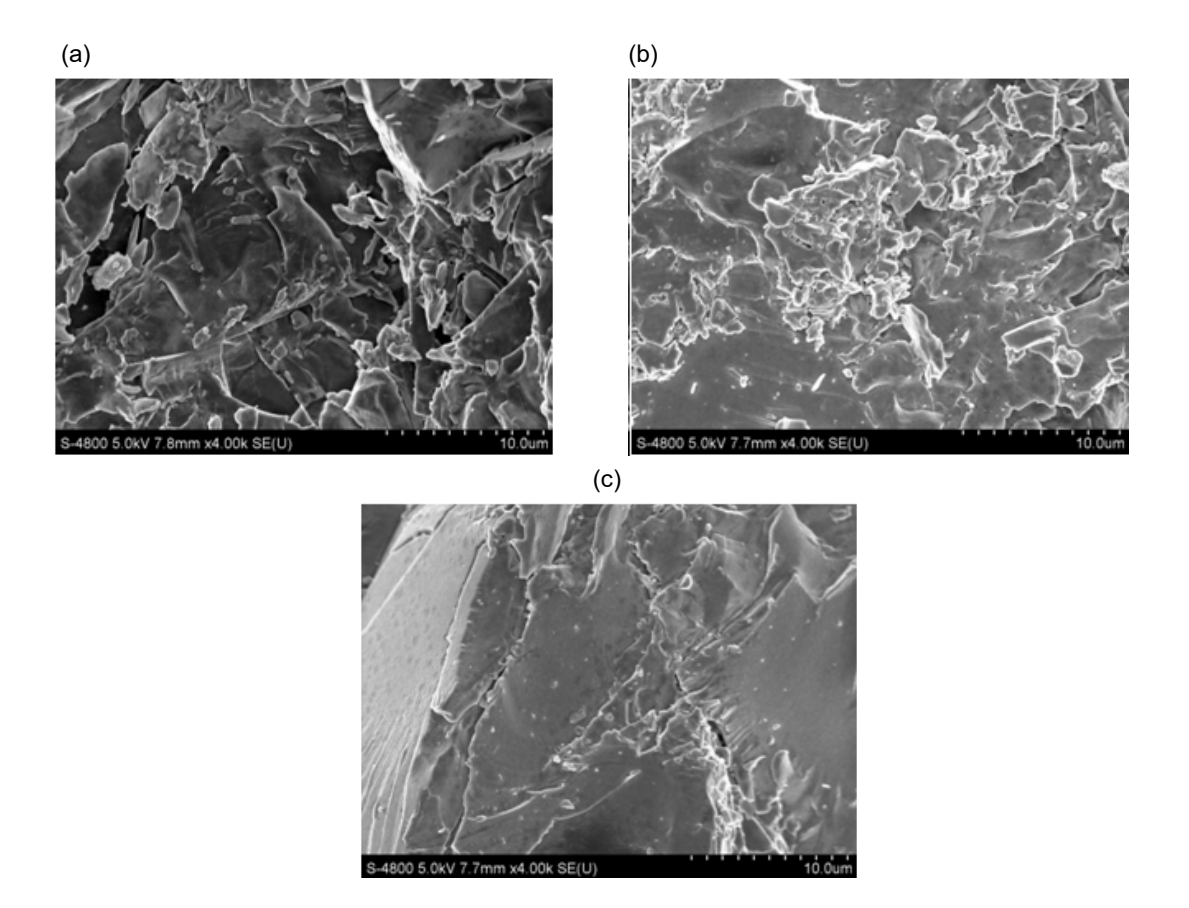


Figure 4 SEM images of the frosted glass plate (a) left-edge side, (b) middle-edge side, and (c) right-edge side (Accelerating voltage of 5kV, emission current of 9000 nA and Magnification of 4k)

2) Possible Chemical Reactions

The most likely chemical pathways that may appear in the DBD system used in this study are proposed as in the following equations (Suttikul *et al.*, 2012-2014).

Active oxygen formation:

$$O_2 + 2e^{-} \rightarrow 2O + 2e^{-}$$
 (5)

Ethylene epoxidation:

$$C_2H_4 + O \rightarrow C_2H_4O$$
 (6)

$$C_2H_4 + 1/2O_2 \quad \rightarrow \qquad C_2H_4O \tag{7}$$

Partial and complete oxidations:

$$C_2H_4 + 2O \longrightarrow 2H_2 + 2CO$$
 (8)

$$C_2H_4 + 4O \longrightarrow 2H_2 + 2CO_2$$
 (9)

$$C_2H_4 + 6O \rightarrow 2H_2O + 2CO_2$$
 (10)

$$C_2H_4 + 2O_2 \rightarrow 2H_2O + 2CO$$
 (11)

$$C_2H_4 + 2O_2 \longrightarrow 2H_2 + 2CO_2$$
 (12)

$$C_2H_4 + 3O_2 \longrightarrow 2H_2O + 2CO_2$$
 (13)

3) Reaction Activity Performance

3.1 Effect of Applied Voltage

CH + CH₂ + 3H

Figure 5 shows the effects of applied voltage on the ethylene epoxidation performance, other product selectivities, and power consumption of the studied DBD system with double frosted glass plates operated at an input frequency of 500 Hz, a feed molar ratio of O_2/C_2H_4 of 0.2:1, an ethylene feed position fraction of 0.5, and a total feed flow rate of 50 cm³/min, according to our previous study (Suttikul *et al.*, 2014). The studied DBD system was only operated in the voltage range of 13-25 kV because an applied voltage below 13 kV could not generate plasma and the O_2 conversion approached 100% at an applied voltage of 25 kV. As shown in Fig. 5a, the C_2H_4 conversion rises with increasing applied voltage, whereas the O_2 conversion increases and reaches 100% at an applied voltage of 25 kV. The C_2H_4 conversion was much lower than the O_2 conversion since the feed molar ratio of O_2/C_2H_4 of 0.2:1 was under an oxygen lean condition (a theoretical malar ratio of O_2/C_2H_4 = 3:1 for complete oxidation).

 C_2H_6

(31)

As shown in Fig. 5b, the EO yield increases remarkably from 0.8 to 10.9% with increasing applied voltage from 13 to 23 kV, and then it adversely decreases to 9.3% with further increasing applied voltage from 23 to 25 kV. The EO selectivity exhibited the same trend as the EO yield. The maximum EO selectivity of 68.2% was found at the same applied voltage of 23 kV which also provided the maximum EO yield of 10.9%. Interestingly, the maximum EO selectivity of 68.2% of the present work was almost the same as compared to that of our previous work (Suttikul *et al.*, 2014), in which an Ag catalyst was loaded on a single glass plate of a DBD system.

Figure 5c shows all other product selectivities as a function of applied voltage. Both CO and CO₂ selectivities varied sinuously with applied voltage. The maximums of both selectivities of 0.61 and 0.54 for CO and CO2, respectively, were found at an applied voltage of 21 kV. The maximums of H2 and C2H6 selectivities were 29.0% and 15.1%, respectively, at the lowest applied voltage of 13 kV and then they tended to decrease with a further increase in the applied voltage over 13 kV. In contrast, the C₃H₈ selectivity steadily increased to reach the highest value of 19.3% at 23 kV. However, the C₃H₈ selectivity decreased when the applied voltage further increased to 25 kV, whereas the CH₄ selectivity was constant in the entire applied voltage range of 13-25 kV. The results can be explained by the fact that the DBD system provided a higher amount of generated energetic electrons with increasing applied voltage from 13 to 25 kV, leading to more opportunities of collisions between C₂H₄ and dissociated O₂ molecules to form EO (eq. 6-7). All other reactions of oxidations, (eq. 8-17), the dehydrogenation (eq. 18-23), cracking reactions (eq. 24-27), and coupling reactions (eq. 29-30) varied insignificantly with applied voltage because the separate feed of C2H4 could lower the opportunity of C2H4 to be collided by generated electrons. Both EO selectivity and yield as well as all other product selectivities decreased when the applied voltage was increased from 23 to 25 kV. This was a result of coke deposition on the glass surface, leading to the reduction of all chemical reaction activities as well as ethylene epoxidation. By performing the carbon balance, the carbon deposit increased from 2-3% in the applied voltage range of 13-23 kV to 6% at the applied voltage of 25 kV. The selectivities for C₂H₄O, CH₄ and other products including C₂H₆, C₃H₈, H₂, CO, and CO₂ decreased at the highest applied voltage of 25 kV, suggesting that a very high applied voltage simply promoted the cracking reactions (eq. 24-27).

The power consumptions per C₂H₄ molecule converted and per EO molecule produced as a function of applied voltage are shown in Fig. 5d. Both power consumptions had an opposite trend with C₂H₄ conversion and EO selectivity (Fig. 5a and Fig. 5b) that increased with increasing applied voltage in the entire range of 13-25 kV. The minimum of the power consumption per EO molecule produced was found at an applied voltage of 23 kV. Therefore, the applied voltage of 23 kV was considered to be an optimum and was selected for the following experiments because it provided the highest ethylene oxide selectivity and yield with the lowest power consumption per EO molecule produced.

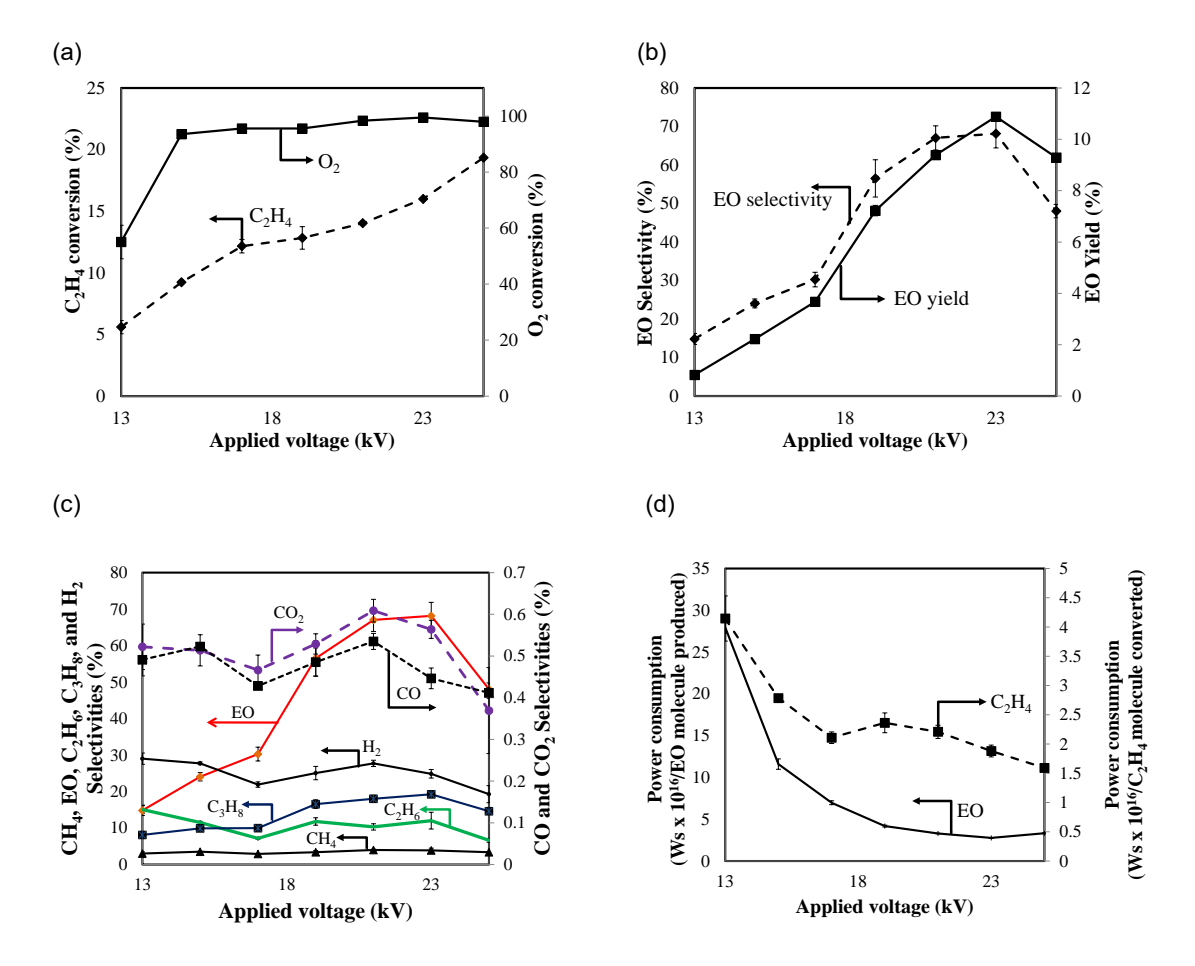


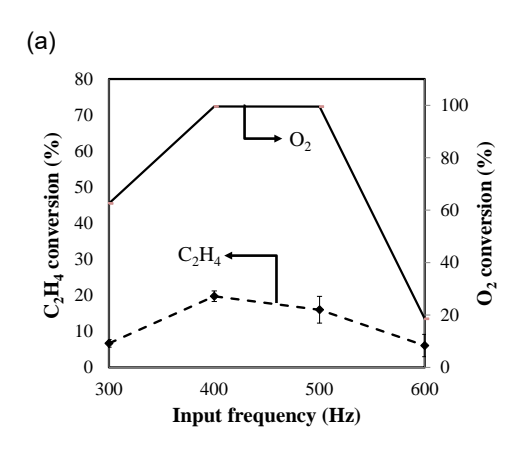
Figure 5 Effect of applied voltage on, (a) C_2H_4 and O_2 conversions, (b) EO selectivity and yield, (c) other product selectivities, and (d) power consumption of the studied DBD system operated at an O_2/C_2H_4 feed molar ratio of 0.2, an input frequency of 500 Hz, C_2H_4 feed position fraction of 0.5, and a total feed flow rate of 50 cm³/min

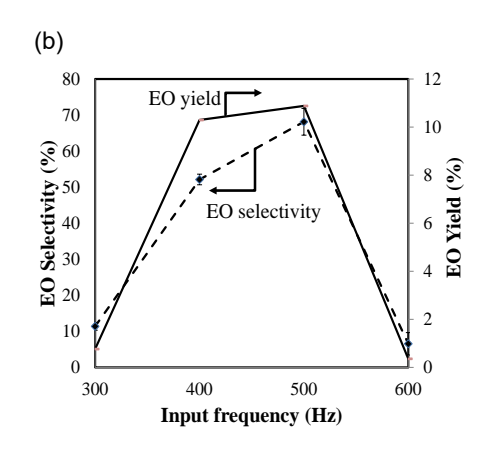
3.2 Effect of Input Frequency

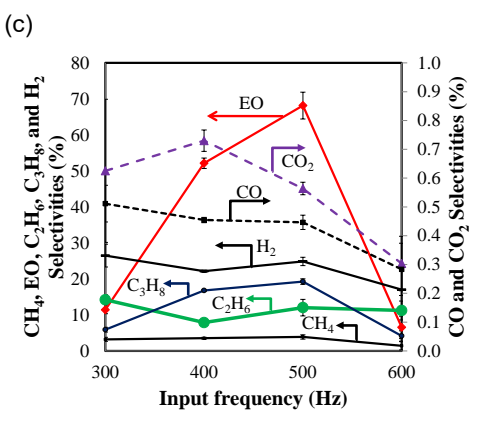
The effect of input frequency on the ethylene epoxidation performance was investigated by varying input frequency from 300 to 600 Hz in which the other operational parameters were fixed at an applied voltage of 23 kV, an O_2/C_2H_4 feed molar ratio of 0.2:1, an C_2H_4 feed position fraction of 0.5, and a total feed flow rate of 50 cm 3 /min. At an input frequency lower than 300 Hz, the generated current was very high, causing a very high temperature to damage the plasma reactor while an input frequency higher than 600 Hz gave unstable plasma. As shown in Fig. 6a, the O_2 conversion increased to 99.5% with increasing input frequency to 400 Hz. The O_2 conversion was nearly unchanged with further increasing of the input frequency from 400 to 500 Hz. Afterwards, it rapidly decreased when input frequency increased over 500 Hz. The effect of input frequency on the C_2H_4 conversion was almost the same as on the O_2 conversion, which increased to reach a maximum at an input frequency of 400 Hz, and then decreased markedly with further increasing input frequency over 400 Hz.

Both EO selectivity and yield rose with increasing input frequency and reached maximum levels at the same input frequency of 500 Hz, as shown in Fig. 6b. Beyond the input frequency of 500 Hz, they sharply dropped with further increasing input frequency from 500 to 600 Hz. The selectivities for other products including CO, CO_2 , CH_4 , C_2H_6 , C_3H_8 , and H_2 as a function of input frequency are shown in Fig. 6c. The selectivities for CO, CO_2 , and H_2 tended to decrease when input frequency increased whereas the CH_4 and C_2H_6 selectivities slightly changed with input frequency. Interestingly, the C_3H_8 selectivity exhibited a similar profile as those of C_2H_4 conversion, EO selectivity and EO yield.

Under the optimum input frequency of 500 Hz, the product selectivities were in the following order: EO >> H_2 > C_3H_8 > C_2H_6 > CH_4 >> CO_2 > CO. The results can be explained by the fact that a decrease in input frequency increased the current (data not shown) to yield a higher number of electrons to be generated, leading to the EO produced to be further oxidized to CO and CO_2 (eq. 15-17), as confirmed experimentally. In contrast, an increase in input frequency from 500 to 600 Hz caused a significant reduction of the current (data not shown), resulting in the lowering of all chemical reactions. As a result, the selectivities of all products decreased greatly when the input frequency increased from 500 to 600 Hz.







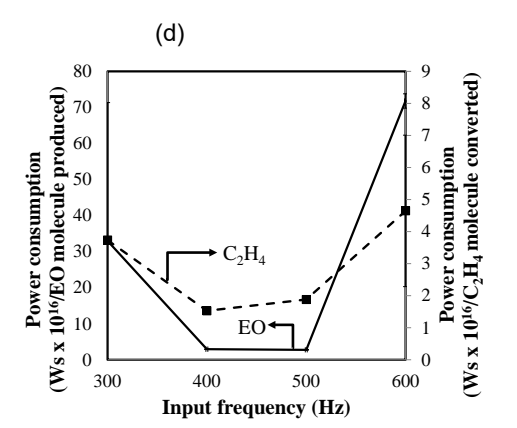


Figure 6 Effect of input frequency on, (a) C_2H_4 and O_2 conversions, (b) EO selectivity and yield, (c) other product selectivities, and (d) power consumption of the studied DBD system operated at an O_2/C_2H_4 feed molar ratio of 0.2, an applied voltage of 23 kV, C_2H_4 feed position fraction of 0.5, and a total feed flow rate of 50 cm³/min

The power consumptions required to convert C_2H_4 and to produce EO as a function of input frequency are shown in Fig. 6d. Both the power consumptions per EO molecule produced and C_2H_4 molecule converted decreased with increasing input frequency to 400 Hz, then remained almost unchanged in the input frequency range of 400-500 Hz, and finally adversely increased when further increasing input frequency from 500 to 600 Hz. The minimum power consumption per EO molecule produced was found at the input frequency of 500 Hz.

From the results, the input frequency of 500 Hz was considered to be optimum for the maximum ethylene epoxidation performance in the DBD system with two frosted glasses and selected for the subsequent experiments.

3.3 Effect of O₂/C₂H₄ Feed Molar Ratio

Figure 7 shows the effect of O_2/C_2H_4 feed molar ratio on the process performance of the studied DBD. The C_2H_4 conversion tended to slightly rise with an increasing O_2/C_2H_4 feed molar ratio. The O_2 conversion rose with an increasing O_2/C_2H_4 feed molar ratio from 0.17 to 0.2 and remained unchanged with a further increasing O_2/C_2H_4 feed molar ratio beyond 0.2. The low C_2H_4 conversion (18-26%) and the high O_2 conversion (>99%) resulted from the system being operated under oxygen lean conditions.

As shown in Fig. 7b, the EO selectivity and yield increased and reach maximum values at the same O2/C2H4 feed molar ratio of 0.2. Beyond the optimum O2/C2H4 feed molar ratio of 0.2, they decreased markedly with an increasing O₂/C₂H₄ feed molar ratio. Interestingly, the selectivities for CH₄, C₂H₆, C₃H₈, and H₂ showed to reach maximum levels at the same O₂/C₂H₄ feed molar ratio of 0.2, except the selectivities for CO and CO2 rose with an increasing O2/C2H4 feed molar ratio. The studied DBD was operated under oxygen lean conditions in order to minimize all undesirable reactions including partial and complete oxidation (eq. 8-17) and cracking reactions (eq. 24-27). When the feed oxygen content was too low (O2/C2H4 feed molar ratio < 0.2), all reactions, including ethylene epoxidation, were found to be very low, indicated by low selectivities for all products including EO. This is because the lower the oxygen content, the lower the active oxygen species to initiate all plasma reactions. When the O₂/C₂H₄ feed molar ratio was greater than 0.2, the selectivities for CO and CO2 rose with an increasing O2/C2H4 feed molar ratio because of the higher oxygen content available for both partial and complete oxidation reactions (eq. 8-17). As a consequence, all other reactions including cracking, coupling, and dehydrogenation as well as decreased from sequent oxidations with an increasing O2/C2H4 feed molar ratio beyond the optimum ratio. The results reveal an oxygen lean condition is one of important process parameters to minimize all unwanted products for the ethylene epoxidation reaction.

As shown in Fig. 7d, the power consumption per C_2H_4 molecule converted mirrors the O_2 conversion whereas the power consumption per EO molecule produced had the opposite tendency. The optimum O_2/C_2H_4 feed molar ratio of 0.2 was selected for further experiments because this ratio provided the highest EO selectivity and yield with reasonably low CO and CO_2 selectivities and lowest power consumption per EO molecule produced.

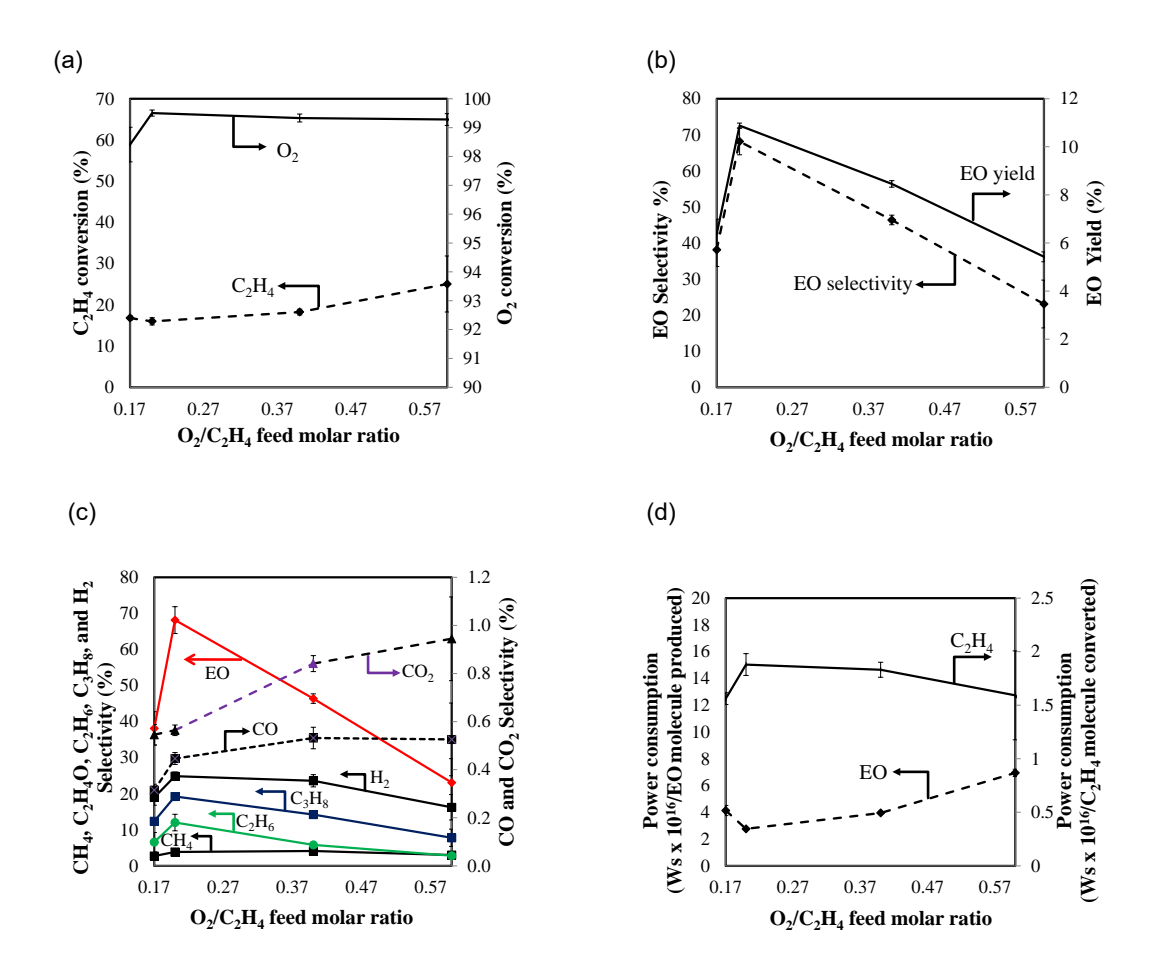


Figure 7 Ethylene epoxidation performance in terms of, (a) C_2H_4 and O_2 conversions, (b) EO selectivity and yield, (c) other product selectivities, and (d) power consumption as function of O_2/C_2H_4 feed malar ratio (an applied voltage of 23 kV, an input frequency of 500 Hz, C_2H_4 feed position fraction of 0.5, and a total feed flow rate of 50 cm³/min)

3.4 Effect of C₂H₄ Feed Position Fraction

As shown in our previous studies (Suttikul *et al.*, 2013), a technique of C_2H_4 separate feed can enhance ethylene epoxidation with significant reduction of undesired reactions (eq. 8-31). Figure 8 shows the process performance of the studied DBD as a function of C_2H_4 feed position fraction. The C_2H_4 feed position fraction was defined according to the flow direction along the electrode length. The O_2 conversion rose with increasing C_2H_4 feed position fraction from 0.4 to 0.5, and after that it decreased with further increasing C_2H_4 feed position fraction. A lower C_2H_4 feed position fraction of 0.5 resulted in more residence time of ethylene in the DBD reactor, leading

to a higher opportunity for ethylene cracking. Moreover, at a C_2H_4 feed position fraction higher than 0.5, the ethylene had a short residence time for epoxidation reaction.

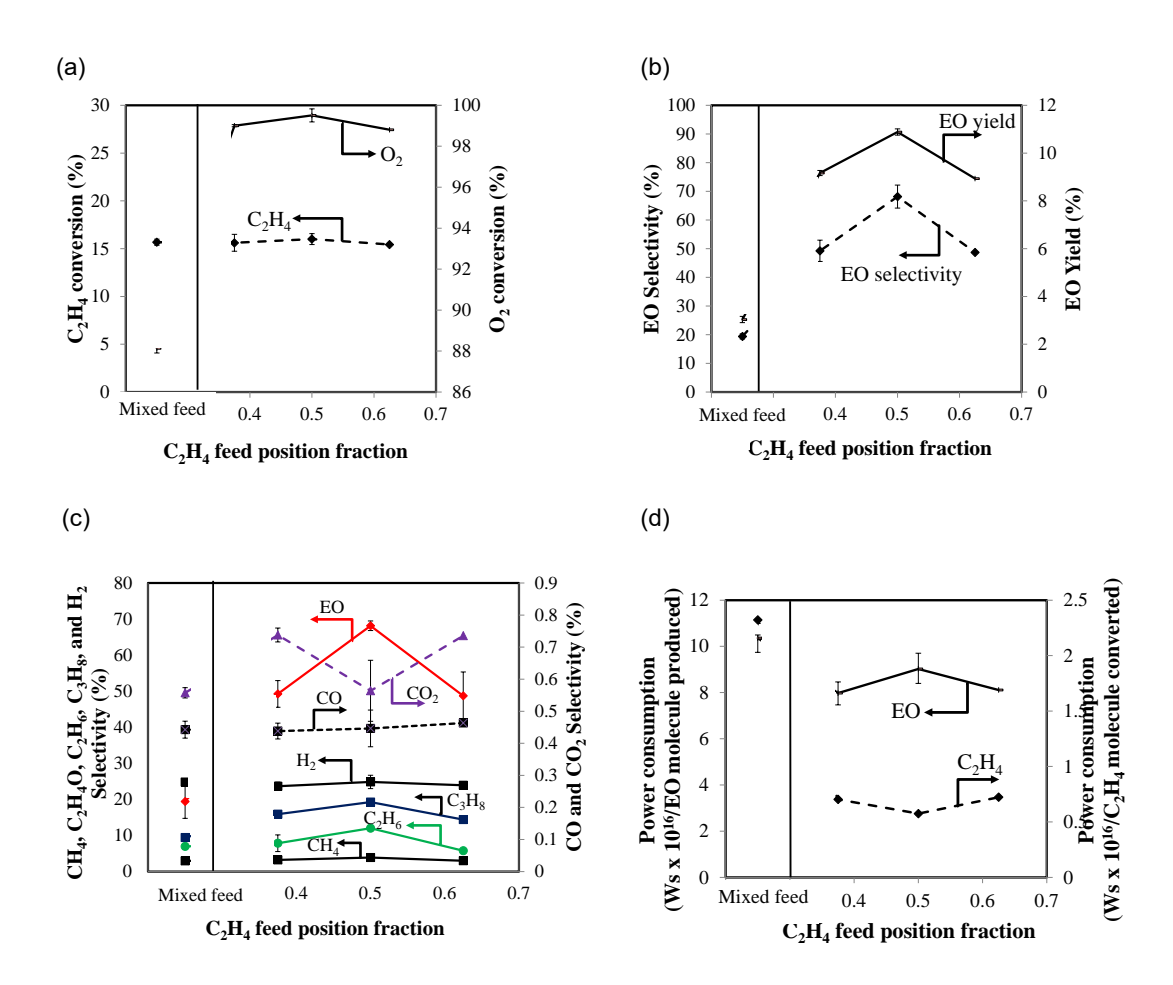


Figure 8 Ethylene epoxidation performance in terms of, (a) C_2H_4 and O_2 conversions, (b) EO selectivity and yield, (c) other product selectivities, and (d) power consumption as function of C_2H_4 feed position fraction (an O_2/C_2H_4 feed molar ratio of 0.2, an applied voltage of 23 kV, an input frequency of 500 Hz, and a total feed flow rate of 50 cm $^3/min$)

3.5 Performance Comparisons of different DBD systems

Table 2 shows a comparison of four DBD systems with a single clear glass plate, 10 wt.% Ag/clear glass plate, two clear glass plates, and two frosted glass plates operated under their own optimum conditions. The DBD system with a single glass plate provided the poorest ethylene epoxidation performance in terms of the lowest EO selectivity with a relatively low EO yield. The use of Ag loaded on a single clear glass plate was found to give the highest EO selectivity of 72.1% with a very low EO yield (1.3%) and C_2H_4 conversion (1.6%). The DBD system with two clear glass plates could only marginally improve EO selectivity (41.3%) with more or less the same EO yield, as compared to that with a single glass plate. Interestingly, the DBD system with two frosted glass plates showed the best process performance in terms of the highest EO yield (10.9%) and the lowest power consumption (2.8x10 $^{-16}$ Ws/EO molecule produced) with a reasonably high EO selectivity. The high surface roughness of two frosted glass plates was found to provide more

uniform micro discharge, leading to the generated electrodes having lower energy than those with either single or two clear glass plates. As known, electrons can emit preferentially from any sharp points or edges than smooth or flat surface. The frosted glass plates provided much more sharp points than a clear glass plate, leading to more uniform plasma with better energy density distribution to be generated. As a result, the use of two frosted glass plates in a DBD system can reduce undesirable reactions especially partial and complete oxidation reactions to form CO and CO_2 which, in turn, enhances the ethylene epoxidation reaction.

Table 2 Comparison of the plasma systems on the ethylene epoxidation performance

Plasma System (conditions)	Conversion (%)		EO selectivity	EO yield	Power consumption (Ws/molecule)			
(Conditions)	C_2H_4	O_2	(%)	(/0/	C ₂ H ₄ converted	EO produced		
Parallel DBD using a clear glass plate (Sreethawong et al., 2008) (Mixed feed, O ₂ /C ₂ H ₄ molar ratio of 1/1, a gap distance of 1 cm, an applied voltage of 19 kV, an input frequency of 500 Hz, and a total feed flow rate of 50 cm ³ /min)	91.0	93.7	6.2	5.6	0.4 x 10 ⁻¹⁶	6.1 x 10 ⁻¹⁶		
Parallel DBD/10 wt.% Ag/glass plate (Suttikul et al., 2014) (Separate feed [C_2H_4 feed position of 0.5], O_2/C_2H_4 molar ratio of 0.2/1, a gap distance of 0.7 cm, an applied voltage of 19 kV, an input frequency of 500 Hz, and a total feed flow rate of $50 \text{ cm}^3/\text{min}$)	1.6	83.0	72.1	1.3	23.0 x 10 ⁻¹⁶	16.6 x 10 ⁻¹⁶		
Parallel DBD using two clear glass plates (This work) (Separate feed $[C_2H_4]$ feed position of 0.5], O_2/C_2H_4 molar ratio of 0.2/1, a gap distance of 0.7 cm, an applied voltage of 19 kV, an input frequency of 500 Hz, and a total feed flow rate of 50 cm ³ /min)	12.7	89.8	41.3	5.2	2.1 x 10 ⁻¹⁶	5.0 x 10 ⁻¹⁶		
Parallel DBD using two frosted glass plates (This work) (Separate feed $[C_2H_4]$ feed position of 0.5], O_2/C_2H_4 molar ratio of 0.2/1, a gap distance of 0.7 cm, an applied voltage of 23 kV, an input frequency of 500 Hz, and a total feed flow rate of 50 cm ³ /min)	19.8	99.5	68.1	10.9	1.9 x 10 ⁻¹⁶	2.8 x 10 ⁻¹⁶		

Conclusion

The optimum conditions for the highest EO product of the DBD system with two frosted glass plates were an applied voltage of 23 kV, an input frequency of 500 Hz, an O_2/C_2H_4 feed molar ratio of 0.2:1, and an C_2H_4 feed position fraction of 0.5. Interestingly, the DBD system using two

frosted glass plates provided a reasonably high EO selectivity and much higher EO yield as compared to the DBD with Ag catalyst loaded on single glass plate. A combination of two frosted glass plates and an Ag catalyst in a DBD system will be investigated in a future study.

Recommendations

The recommendations for future work are as follows:

- Methane is commercially used as a balancing gas in conventional catalytic processes. The
 ethylene epoxidation should be investigated in a low-temperature plasma system to clearly
 understand about the role of methane on the chemical pathways and how it affects the plasma
 system.
- 2. The gap distance between two electrodes of a DBD reactor is one of the most parameters that significantly affect the plasma behavior. To study the effect of the gap distance, corresponding to the plasma volume and residence time is of interest.

References

- Campbell, C. T. (1986). Chlorine promoters in selective ethylene epoxidation over Ag(111): A comparison with Ag(110). Journal of catalysis, 99(1), 28-38.
- Epling, W. S., Hoflund, G. B., and Minahan, D. M. (1997). Study of Cs-promoted, α-alumina-supported silver, ethylene-epoxidation catalysts. <u>Journal of catalysis</u>, 171(2), 490-497.
- Geenen, P. V., Boss, H. J., and Pott, G. T. (1982). A study the vapor-phase epoxidation of propylene and ethylene on silver and silver-gold alloy catalysts. <u>Journal of catalysis</u>, 77, 499-510.
- Goncharova, S. N., Paukshtis, E. A., and Bal'zhinimaev, B. S. (1995). Size effects in ethylene oxidation on silver catalysts: influence of support and Cs promoter. <u>Applied catalysis A: general</u>, 126, 67-84.
- Jankowiak, J. T., and Barteau, M. A. (2005). Ethylene epoxidation over silver and coppersilver bimetallic catalysts: I. Kinetics and selectivity. <u>Journal of catalysis</u>, 236(1), 366-378.
- Jankowiak, J. T., and Barteau, M. A. (2005). Ethylene epoxidation over silver and copper-silver bimetallic catalysts: II. Cs and Cl promotion. <u>Journal of catalysis</u>, 236(1), 379-386.
- Mendes, G. C. C., Brandaõ, T. R. S., and Silva, C. L. M. (2007). Ethylene oxide sterilization. American journal of infection control, 35, 574-581.
- Patiño, P., Ropero, M., and Iacocca D. (1996). Reactions of O(³P) with aromatic compounds in liquid phase. <u>Plasma Chemistry and Plasma Processing</u>, 16(4), 563-575.
- Pietruszka, B., and Heintze, M. (2004). Methane conversion at low temperature: the combined application of catalysis and non-equilibrium plasma. <u>Catalysis today</u>, 90, 151-8.

- Rosacha, L. A., Anderson, G. K., Bechtold, L. A., Coogan, J. J., Heck, H. G., Kang, M., McCulla, W. H., Tennant, R. A., and Wantuck, P. J. (1993). Treatment of hazardous organic wastes using silent discharge Plasmas. Non-Thermal Plasma Technique for Pollution Control, NATO ASI series, 34, part B, 128-139.
- Rueangjitt, N., Sreethawong, T., Chavadej S., and Sekiguchi H. (2011) Non-Oxidative Reforming of Methane in a Mini-Gliding Arc Discharge Reactor: Effects of Feed Methane Concentration, Feed Flow Rate, Electrode Gap .Distance, Residence Time, and Catalyst Distance. Plasma Chemistry and Plasma Processing, 31, 517–534.
- Sreethawong, T., Permsin, N., Suttikul, T., Chavadej, S. (2010) Ethylene Epoxidation in Low-Temperature AC Dielectric Barrier Discharge: Effect of Electrode Geometry. <u>Plasma</u> Chemistry and Plasma Processing, 30(4), 503-524.
- Sreethawong, T., Suwannabart, T., and Chavadej, S. (2008) Ethylene epoxidation in low-temperature AC dielectric barrier discharge: Effects of oxygen-to-ethylene feed molar ratio and operating parameters. Plasma Chemistry and Plasma Processing, 28(5), 629-642.
- Sreethawong, T., Suwannabart, T., and Chavadej, S. (2009) Ethylene Epoxidation in Low-Temperature AC Corona Discharge over Ag Catalyst: Effect of Promoter. Chemical Engineering Journal, 115(1-2), 396-403.
- Suhr, H., and Pfreundschuh, H. (1988). Reactions of nonequilibrium oxygen plasmas with liquid olefins. Plasma chemistry and plasma processing, 8(1), 67-74.
- Suhr, H., Schmid, H., Pfeundschuh, H., and Lacocca, D. (1984). Plasma oxidation of liquids. Plasma chemistry and plasma processing, 4(4), 285-295.
- Suttikul, T., Paosombat, B., Santikunaporn, M., Leethochawalit, M., and Chavadej, S. (2014)
 Improvement of Ethylene Epoxidation in a Parallel Plate Dielectric Barrier Discharge
 System by Ethylene/Oxygen Separate Feed and Ag Catalyst. Industrial and Engineering
 Chemistry Research, 53, 3778—3786
- Suttikul, T., Sreethawong, T., Segiguchi, H. and Chavadej, S. (2011). Ethylene epoxidation over alumina-and silica-supported silver catalysts in low-temperature AC dielectric barrier discharge. Plasma chemistry and plasma processing, 31, 273-290.
- Suttikul, T., Suttikul, T., Yaowapong-aree, S., Sekiguchi, H., Chavadej, S., and Chavadej, J. (2013)
 Improvement of ethylene epoxidation in low-temperature corona discharge by separate ethylene/oxygen feed. Chemical Engineering and Processing: Process Intensification, 70, 222-232
- Suttikul, T., Tongurai, C., Sekiguchi, H., and Chavadej, S. (2012) Ethylene epoxidation in cylindrical dielectric barrier discharge: Effects of separate ethylene/oxygen feed. Plasma Chemistry and Plasma Processing, 32, 1169-1188
- Thomas, F.O., Corke, T.C., Iqbal, M., Kozlov, A., and Schatzman, D. (2009) Optimization of Dielectric Barrier Discharge Plasma Actuators for Active Aerodynamic Flow Control. <u>The</u> American Institute of Aeronautics and Astronautics, 47, 2169-2178.

Watkinson, C. (2007). Improving the reliability of mechanical seals in ethylene oxide applications.

<u>Sealing Technology</u>, 12, 8-12.

Output จากโครงการวิจัยที่ได้รับทุนจาก สกว.

- 1. ผลงานตีพิมพ์ในวารสารวิชาการนานาชาติ (ระบุชื่อผู้แต่ง ชื่อเรื่อง ชื่อวารสาร ปี เล่มที่ เลขที่ และหน้า) หรือผลงานตามที่คาดไว้ในสัญญาโครงการ
 - 1) Chavadej, S., Dulyalaksananon, W. and Suttiku,I T. (2016) Ethylene epoxidation in a low-temperature parallel plate dielectric barrier discharge system with two frosted glass plates. Chemical Engineering and Processing: Process Intensification, 107, 127–137. (ภาคผนวก A)
 - 2) Suttiku,I T. and Chavadej, S. (2017) Ethylene Epoxidation in a Low-Temperature Parallel Plate Dielectric Barrier Discharge System: Effect of Oxygen Source. Industrial and Engineering Chemistry Research, 56, 12547-12555. (ภาคผนวก B)
- 2. การนำผลงานวิจัยไปใช้ประโยชน์เชิงวิชาการ
 - มีการนำผลการวิจัยไปใช้พัฒนาการเรียนการสอน โดย สาขาวิชาเทคโนโลยี วิศวกรรมกระบวนการเคมี คณะวิศวกรรมศาสตร์และเทคโนโลยี มหาวิทยาลัย เทคโนโลยีพระจอมเกล้าพระนครเหนือ และสถาบันการศึกษาต่างๆ
 - ผลที่ได้จากโครงการ "การศึกษาปฏิกิริยาเอทธิลีนอีพอกซิเดชันในระบบ ประกายไฟฟ้าพลาสมา" สามารถสร้างองค์ความรู้ใหม่ (Journal paper) และ ผลิตบุคลากรทางด้านวิศวกรรมเคมีที่มีความเชี่ยวชาญด้านปฏิกิริยาเคมีของ ประเทศ สามารถนำองค์ความรู้ใหม่ไปประยุกต์สร้างเครื่องต้นแบบต่อไป

Appendix

- A. Ethylene epoxidation in a low-temperature parallel plate dielectric barrier discharge system with two frosted glass plates
- B. Ethylene Epoxidation in a Low-Temperature Parallel Plate Dielectric Barrier Discharge System: Effect of Oxygen Source

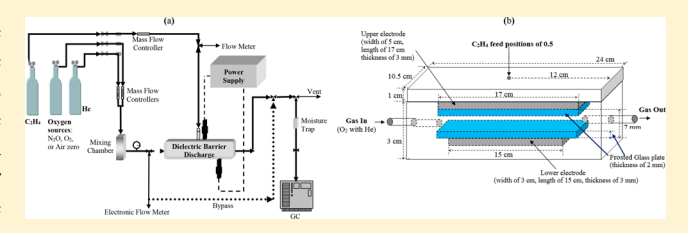


Cite This: Ind. Eng. Chem. Res. 2017, 56, 12547-12555

Ethylene Epoxidation in a Low-Temperature Parallel Plate Dielectric Barrier Discharge System: Effect of Oxygen Source

Thitiporn Suttikul[†] and Sumaeth Chavadej*,^{‡,§}

ABSTRACT: The objective of this work was to investigate the effects of two different oxidizing agents [nitrous oxide (N_2O) and air], compared to the reported pure oxygen (O_2) , on the ethylene epoxidation performance in a low-temperature parallel plate dielectric barrier discharge (DBD) system with two frosted glass plates as the dielectric barrier material under ambient temperature and atmospheric pressure. A separate feed technique, with the ethylene (C2H4) feed position



fraction of 0.5, was used to reduce all the undesirable reactions and to maximize the ethylene oxide (EO) production (selectivity and yield). The N₂O system with a N₂O/C₂H₄ feed molar ratio of 0.17:1 exhibited the highest ethylene epoxidation performance (80.1% EO selectivity and 21.9% EO yield) with a very low carbon monoxide selectivity and the lowest power consumption, as compared to pure O_2 and air as oxidant systems at their respective optimal feed molar ratios of 0.2:1 and 0.1:1, respectively. Interestingly, the EO yield from the DBD system with N2O was about 2-fold higher than that of the O2 and air system.

1. INTRODUCTION

Ethylene epoxidation uses molecular oxygen to react with ethylene (C_2H_4) to produce ethylene oxide (EO), as discovered by Lefort in 1931, an important industrial chemical that is used as a feedstock for the production of various useful chemicals such as surfactants, sterilants for food, solvents, antifreeze and adhesives, leading to a high demand for EO.^{2,3} Currently, EO is commercially produced from the partial oxidation of C₂H₄, the so-called ethylene epoxidation reaction, over silver catalysts loaded on a low surface area alumina (α -Al₂O₃) support with a reasonably high EO selectivity.^{4,5} Transition metal promoters, such as Pd, Cs, Cu, Re, and Au, and the cofeeding of chlorinecontaining moderators into the gaseous reactants have been used to improve the EO production performance, 6-12 where C₂H₄ in the gas phase reacts with the adsorbed molecular oxygen on the silver surface to form EO. However, conventional catalytic processes still require both a high temperature and pressure operation which, in turn, results in catalyst deactivation from coke deposition, agglomeration of catalyst particles, and sintering of metal sites, causing a significant reduction in the catalytic activity. Therefore, the search for a new technique operated at ambient temperature and atmospheric pressure with a lower-energy consumption is of great interest.

Nonthermal plasma is one promising technique that can be employed in various applications. Dielectric barrier discharge (DBD) is a type of nonequilibrium low temperature plasma that has high electron temperatures (10⁴-10⁵ K) with a bulk gas temperature close to room temperature. 13,14 As a consequence, the energy consumption used for operating the plasma system for various chemical reactions is lower compared to conventional catalytic processes. Accordingly, DBD has been employed for several studies, including chemical synthesis, such as hydrogen (H₂) production by methane (CH₄) reforming¹⁵⁻²³ and ethylene epoxidation,²⁴⁻²⁹ ozone generation,³⁰⁻³² soil remediation, ^{33–37} wastewater treatment, ^{38,39} and surface treatment.

For the gas-phase ethylene epoxidation, the molar ratio of oxygen (O2) to C2H4 significantly affects the pathway reactions.44 Fundamentally, the oxidative combustion of hydrocarbons occurs with excess O2, while partial oxidation, especially ethylene epoxidation, markedly occurs under a lean O₂ condition. ^{24-27,29,45} Both the type and amount of oxygen species have been reported to affect the chemical reactions. Studies of alternative oxidants in the form of various oxygencontaining molecules, such as nitrous oxide (N2O), O2, and hydrogen peroxide (H2O2) were investigated for a number of chemical reactions, including propylene epoxidation. 46-52 Hence, N2O was, for the first time of its kind, investigated for the ethylene epoxidation reaction in the present study.

August 30, 2017 Received: September 28, 2017 Revised: Accepted: October 12, 2017 Published: October 12, 2017

[†]Division of Chemical Process Engineering Technology, Faculty of Engineering and Technology, King Mongkut's University of Technology North Bangkok, Rayong Campus, Rayong 21120, Thailand

[‡]The Petroleum and Petrochemical College, Chulalongkorn University, Soi Chula 12, Phyathai Road, Pathumwan, Bangkok 10330, Thailand

[§]Center of Excellence on Petrochemical and Materials Technology, Chulalongkorn University, Bangkok 10330, Thailand

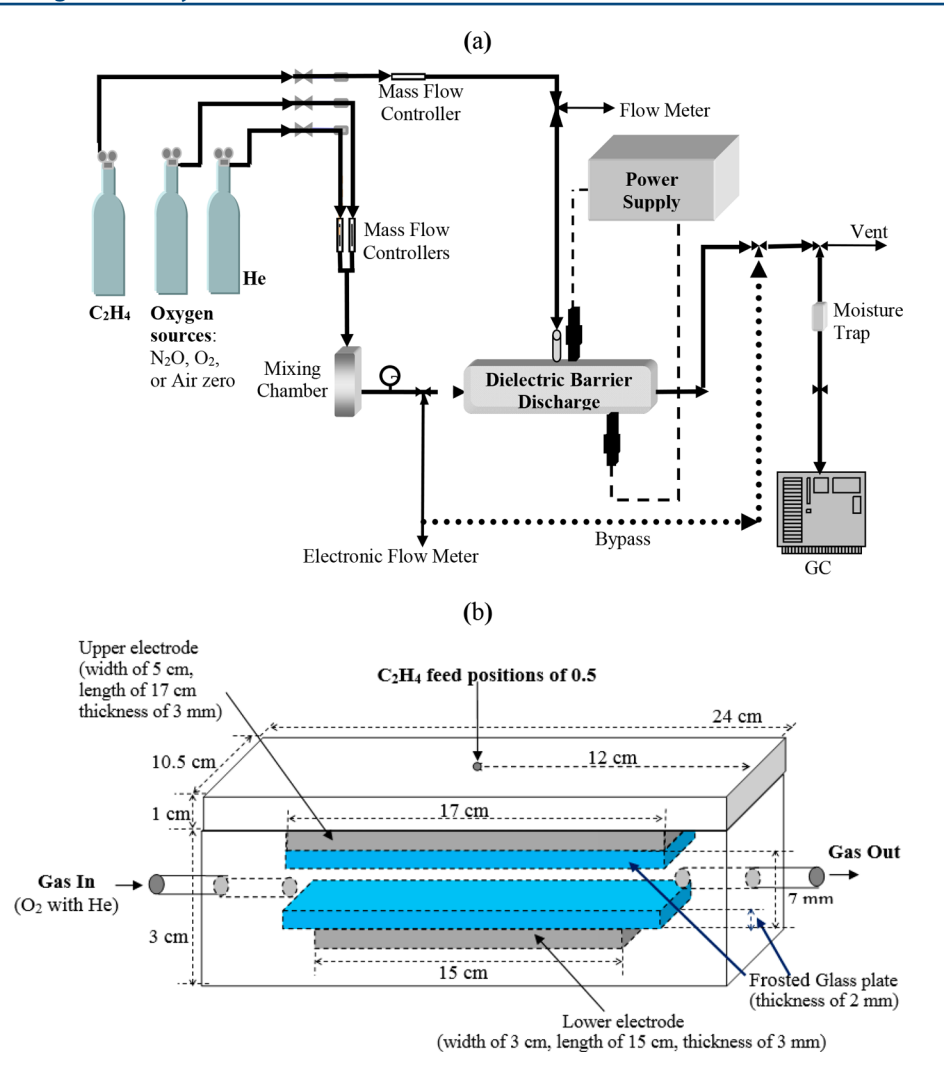


Figure 1. (a) Schematic diagram of the experimental setup of the DBD plasma system for the ethylene epoxidation reaction and (b) configuration of the parallel plate DBD reactor with two frosted glass plates.

In this work, the ethylene epoxidation was investigated in a low-temperature parallel plate DBD with two frosted glass plates and a separate feed of C_2H_4 and the oxidant (air or N_2O) to reduce the undesired combustion reactions and to enhance ethylene epoxidation performance, as previously reported. Two oxidizing agents (N_2O and air) were tested for the ethylene epoxidation reaction, and compared to that previously reported for pure oxygen (O_2) in the same system and conditions, thill the effects of the oxidant/ C_2H_4 feed molar ratio on the ethylene epoxidation performance were studied. Finally, under the evaluated optimum feed ratio of each system, the EO production performance in terms of C_2H_4 and oxidant conversions, EO selectivity and yield, selectivity for other products, and power consumption were compared.

2. EXPERIMENTAL SECTION

2.1. Chemical and Gases for Reaction Experiments. 97% N_2O with helium balance ($\pm 1\%$ uncertainty) and air zero [high purity grade; 20.5% (v/v) O_2 and 79.5% (v/v) N_2] were used as the oxygenating sources to react with 40% C_2H_4 with helium balance ($\pm 1\%$ uncertainty) at different feed molar ratios, all with 99.995% helium (high purity grade) as the balancing gas and at a desired total flow rate of 50 cm³/min to avoid flammability limits for safety. All reactant gases were

specially blended by Thai Industrial Gas Co., Ltd. and used without any purification. Two frosted glass plates of 2 mm thickness were placed on the surface of both stainless-steel plate electrodes as dielectric barrier sheets to form the DBD reactor. Both frosted glass plates were cleaned with distilled water and acetone a few times before use.

2.2. Experimental Setup and Reaction Activity Experiments. The gas-phase experiments were performed in a parallel plate DBD reactor with two frosted glass plates, which were operated at an applied voltage of 23 kV, an input frequency of 500 Hz, the stated O₂ (in air)/C₂H₄, or N₂O/ C_2H_4 feed molar ratio with a C_2H_4 feed position fraction of 0.5, being the optimum conditions obtained previously for pure ⁴ To minimize all the undesirable reactions of carbon monoxide (CO) formation, carbon dioxide (CO₂) formation, dehydrogenation, coupling and cracking, the C₂H₄ reactant was injected at the middle of the top electrode length (a C₂H₄ feed position fraction of 0.5), while the air or N₂O was fed throughout the electrode length. The schematic diagram of the DBD system showing the details of the DBD reactor configuration are shown in Figure 1. The DBD reactor was comprised: (i) an acrylic box of inner dimensions of 5.5 cm wide × 17.5 cm long × 2.0 cm high and outer dimensions of 10.5 cm wide \times 24.0 cm long \times 3.0 cm high; (ii) two different

sizes of the stainless steel-made electrode rectangles of 3.0 cm wide \times 15.0 cm long \times 0.3 cm thick for the bottom electrode and 5.0 cm wide × 17.0 cm long × 0.3 cm thick for the top electrode; (iii) two frosted glass plates of 5.5 cm wide × 17.5 cm long × 0.2 cm thick. The gap distance between the two electrodes was fixed at 7 mm. Microdischarge was generated by applying an alternating current (AC) across the electrodes at an applied voltage of 23 kV and a frequency of 500 Hz, which were previously found to be the optimum conditions.²⁴ A domestic AC power (220 V, 50 Hz supply) was converted to high voltage AC by a three-step power supply system, as described previously.⁵³ The output voltage and frequency of the high voltage AC were adjusted by a function generator, and its sinusoidal wave signal was monitored by an oscilloscope. The input power and current of the DBD system were measured by a power analyzer (Extech Instruments Corporation, True RMS Single Phase Power Analyzer, 380801), whereas the output voltage was measured by a digital multimeter (Agilent, U1273A) with a high voltage probe (Cal Test Electronics, CT2700).

The molecular oxygen source (N2O or air) balanced with helium was fed through the DBD reactor while C2H4 was separately injected at the middle electrode length. For the air system, the amount of O2 in the air zero was used to compute for O_2/C_2H_4 feed molar ratio, while the amount of N_2 in the air zero was combined with the amount of the helium to keep a total feed flow rate of 50 cm³/min. Electronic mass flow controllers, supplied by AALBORG Instruments & Controls Inc., were used to control all gases to get the desired feed gas mixture. A 7-µm in-line filter was placed upstream of each mass flow controller in order to trap any foreign particles, while a check valve was placed downstream of each mass flow

controller to prevent any back flow of gas. The DBD reactor was operated at ambient temperature (25-27 °C) and atmospheric pressure, which was controlled via a needle valve. The outlet gas was either vented to the atmosphere via an exhaust rubber tube or allowed to flow through an online gas chromatograph (GC; PerkinElmer, AutoSystem) to detect the product gas composition. The moisture in the effluent gas was removed by a water trap filter before entering the online GC. The compositions of the feed and outlet gas were determined by GC, equipped with a thermal conductivity detector (TCD) and a flame ionization detector (FID). For the TCD channel, a capillary column (HP-PLOT Molesieve) was used to separate the product gases, including H_2 , O_2 , nitrogen (N_2) , CO, CO_2 , and N₂O. For the FID channel, a capillary column (OV-Plot U) was used for the analysis of EO and other byproduct gases, such as CH_4 , acetylene (C_2H_2) , ethane (C_2H_6) , and propane (C₃H₈). After the feed composition was unchanged with time, the power supply was turned on to generate the discharges. The product gas composition was analyzed by the GC every 25 min (at least three times). The experimental data with less than 5% error were averaged and then used to determine the DBD system performance in terms of the C₂H₄ and the O2 or N2O conversion levels and all product selectivities, including those for EO, H₂, CH₄, C₂H₆, C₂H₂, C₃H₈, CO, and CO₂, plus the EO yield. These were computed using eqs 1-3):

% reactant conversion

$$= \frac{\text{(moles of reactant in - moles of reactant out)} \times 100}{\text{(moles of reactant in)}}$$
(1)

$$\text{\% product selectivity} = \frac{\left[(\text{number of carbon or hydrogen atom in product})(\text{moles of product produced}) \right] \times 100}{\left[(\text{number of carbon or hydrogen atom in C}_2\text{H}_4)(\text{moles of C}_2\text{H}_4 \text{ converted}) \right]}$$

%EO yield =
$$[(%C_2H_4 \text{ conversion}) \times (%EO \text{ selectivity})]/100$$
 (3

In addition, the power consumption was calculated, in terms of W s per C₂H₄ molecule converted or per EO molecule produced, using eq 4,

power consumption =
$$(P \times 60)/(N \times M)$$
 (4)

where P is the power (W), N is Avogadro's number (6.02 \times 10^{23} molecules/mol), and M is the rate of converted C_2H_4 molecules in the feed or rate of produced EO molecules (mol/

The obtained results for the air and N₂O systems were then indirectly compared with the previously published results for pure O_2 in the same system under the same conditions.²⁴

3. RESULTS AND DISCUSSION

3.1. Possible Chemical Reactions. It is worthwhile to point out that under the studied conditions of both the air and N2O systems, CO2 was not detected and so all reactions to form CO₂ can be excluded. Most of the possible chemical pathways that may appear in the DBD system used in this study are proposed in eqs 5-37, as previously reported. 54-58

Active oxygen species formation:

$$N_2O + e \rightarrow 1/2O_2 + N_2 + e$$
 (5)

$$O_2 + e \rightarrow 2O + e \tag{6}$$

Ethylene epoxidation:

$$C_2H_4 + N_2O \rightarrow C_2H_4O + N_2$$
 (7)

$$C_2H_4 + 1/2O_2 \rightarrow C_2H_4O$$
 (8)

$$C_2H_4 + O \rightarrow C_2H_4O \tag{9}$$

Partial oxidations:

$$C_2H_4 + 4N_2O \rightarrow 2CO + 2H_2O + 4N_2$$
 (10)

$$C_2H_4 + 2O_2 \rightarrow 2CO + 2H_2O$$
 (11)

$$C + O \to CO \tag{12}$$

Oxidative dehydrogenation:

$$C_2H_4 + 2N_2O \rightarrow 2CO + 2H_2 + 2N_2$$
 (13)

$$C_2H_4 + O_2 \rightarrow 2CO + 2H_2$$
 (14)

$$C_2H_4 + 2O \rightarrow 2CO + 2H_2$$
 (15)

$$C_2H_4O + N_2O \rightarrow 2CO + 2H_2 + N_2$$
 (16)

$$C_2H_4O + 1/2O_2 \rightarrow 2CO + 2H_2$$
 (17)

Industrial & Engineering Chemistry Research

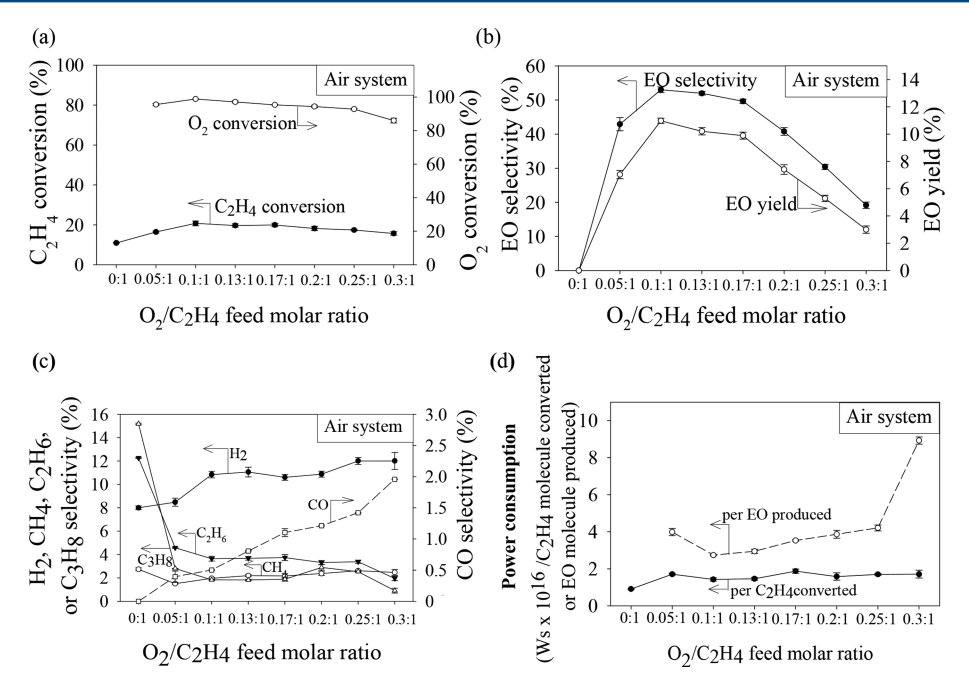


Figure 2. Effect of the O_2 (in air)/ C_2H_4 feed molar ratio on the (a) C_3H_4 and O_2 conversion levels, (b) EO selectivity and yield, (c) other product selectivities, and (d) power consumption. Applied voltage of 23 kV, input frequency of 500 Hz, C2H4 feed position fraction of 0.5, and total feed flow rate of 50 cm³/min.

(24)

$$C_2H_4O + O \rightarrow 2CO + 2H_2$$
 (18)
 $C_2H_3 + 2O \rightarrow 2CO + 3H$ (19)
Water spitting:
 $H_2O + 2e \rightarrow O + H_2 + 2e$ (20)
 $H_2O + 2e \rightarrow OH + H + 2e$ (21)
 $H_2O + 2e \rightarrow O + 2H + 2e$ (22)
Hydrogen spitting
 $H_2 + 2e \rightarrow 2H + 2e$ (23)

 $H_2 + 2e \rightarrow 2H + 2e$

 $C_2H_4 + 4e \rightarrow 2C + 4H + 4e$

$$C_2H_4 + e \rightarrow 2CH_2 + e \tag{25}$$

$$CH_2 + e \rightarrow CH + H + e \tag{26}$$

$$CH + e \rightarrow C + H + e \tag{27}$$

$$C_2H_4 + e \rightarrow CH_4 + C \tag{28}$$

Coupling:

$$C_2H_3 + H \rightarrow C_2H_4 \tag{29}$$

$$CH_2 + C_2H_4 + 2H \rightarrow C_3H_8$$
 (30)

$$2CH_3 \rightarrow C_2H_6 \tag{31}$$

$$CH_4 + CH_2 \rightarrow C_2H_6 \tag{32}$$

$$2CH_2 \rightarrow C_2H_4 \tag{33}$$

$$4CH_2 \rightarrow C_4H_8 \tag{34}$$

$$2C_2H_4 \to C_4H_8$$
 (35)

$$4CH_2 + 2H \rightarrow C_4H_{10}$$
 (36)

$$2CH + 2CH_4 \rightarrow C_4H_{10}$$
 (37)

3.2. Reaction Activity Performance. 3.2.1. Air System. The air used as an oxidative reactant in the studied DBD system principally contains 20.5% (v/v) O₂ and 79.5% (v/v) N₂. The air system was operated at the same operational conditions as previously reported for the O₂ system, ²⁴ which were an applied voltage of 23 kV, input frequency of 500 Hz, C₂H₄ feed position fraction of 0.5, and a total feed flow rate of 50 cm³/min (a residence time of 0.81 min), while the O₂ (in air)/C₂H₄ feed molar ratio was varied from 0:1 to 0.3:1. Figure 2 illustrates the air system performance for the ethylene epoxidation reaction as a function of the O_2/C_2H_4 feed molar ratio. The O₂ conversion level increased slightly with increasing O₂/C₂H₄ feed molar ratios from 0.05:1 to 0.1:1 but then decreased when further increasing the O2/C2H4 feed molar ratio from 0.1:1 to 0.3:1. The C₂H₄ conversion level significantly increased with increasing O₂/C₂H₄ feed molar ratio from 0:1 to 0.1:1 and then slightly decreased when further increasing the O_2/C_2H_4 feed molar ratios from 0.1:1 to 0.3:1. As expected, the O2 conversion level was markedly higher than that for C₂H₄, because the bond dissociation energy of O₂ (498.34 kJ/mol) is much lower than that of C₂H₄ (682 kJ/ mol), leading to O2 molecules being broken down more easily than C₂H₄ molecules by the electron collision.

As shown in Figure 2b, both the EO selectivity and yield drastically increase with increasing O₂/C₂H₄ feed molar ratios up to 0.1:1 and then greatly decrease with further increases in the O₂/C₂H₄ feed molar ratio. Hence the maximum EO selectivity and yield were found at an O₂/C₂H₄ feed molar ratio of 0.1:1, which corresponded well to the maximum C₂H₄ and O2 conversion levels. The CO selectivity steadily increased as the O₂/C₂H₄ feed molar ratio increased and reached a maximum at the highest O₂/C₂H₄ feed molar ratio of 0.3:1, while the H₂ selectivity tended to increase with increasing O₂/ C₂H₄ feed molar ratios (Figure 2c). The increased CO selectivity with the increased O2/C2H4 feed molar ratio can **Industrial & Engineering Chemistry Research**

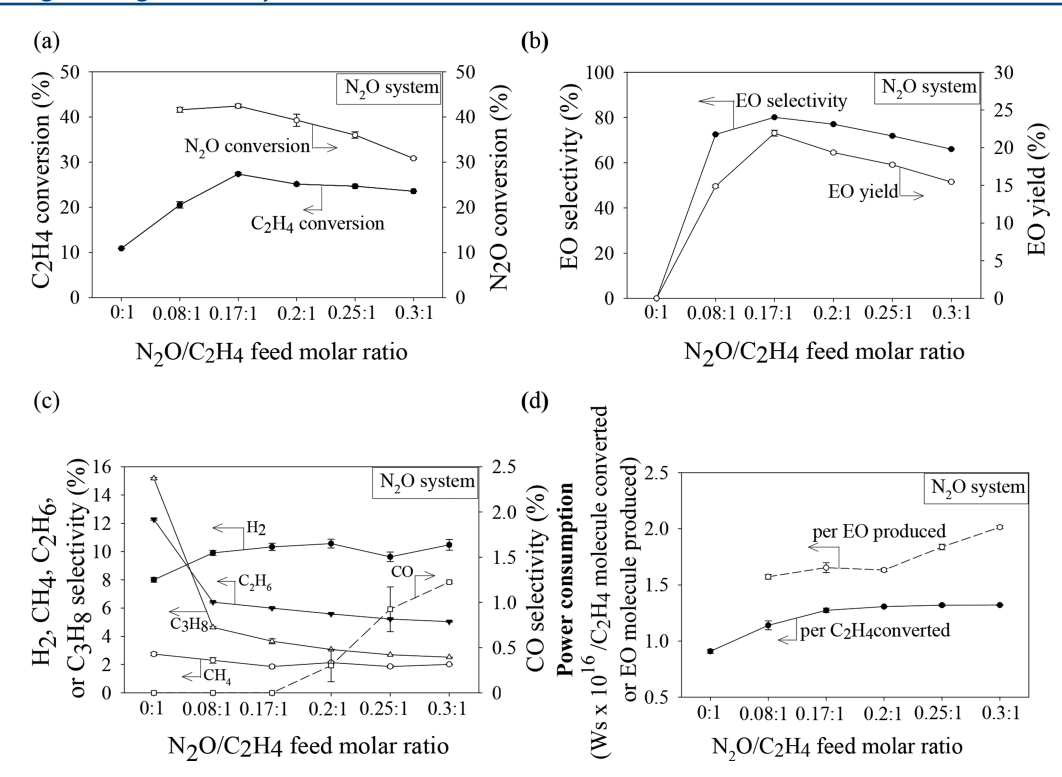


Figure 3. Effect of the N_2O/C_2H_4 feed molar ratio on the (a) C_2H_4 and N_2O conversion levels, (b) EO selectivity and yield, (c) other product selectivities, and (d) power consumption. Applied voltage of 23 kV, input frequency of 500 Hz, C_2H_4 feed position fraction of 0.5, and total feed flow rate of 50 cm³/min.

be explained by the fact that the increase in oxygen would promote the partial oxidation and oxidative hydrogentation reactions (eqs 11, 12, 14, 15, and 17-19). The results also indicated that the O₂/C₂H₄ feed molar ratio slightly influenced the cracking reactions (eqs 24-28) and coupling reactions (eqs 29-33), supported by the low selectivities for CH₄, C₂H₆, and C₃H₈. Except in the absence of O₂, the coupling reactions for the formation of C₂H₆ and C₃H₈ were predominant (Figure 2c). The C_2H_6 and C_3H_8 selectivities were 12.3 and 15.2%, respectively, with no produced CO and CO₂ (the absence of O₂), while the C₂H₆ and C₃H₈ selectivities slightly changed in the range of 2.0-3.7% and 0.9-2.9%, respectively (the presence of O₂). The presence of oxygen from added air caused the dominance of all reactions of oxidative dehydrogenation (eq 13-19), partial oxidation (eq 10-12), and ethylene epoxidation (eq 7-9) with the reduction of the coupling reactions. Interestingly, in the presence of O2, the H2 selectivity was found to be the second highest product, suggesting that H₂ production mainly resulted from oxidative dehydrogenation reactions (eqs 14 and 15). The results indicated that increasing the amount of active oxygen species can promote partial oxidations (eqs 11 and 12) and oxidative dehydrogenation reactions (eqs 14, 15, and 17–19) to form coke, CO, and H_2 . A lean oxygen condition is required to maximize the EO formation with a minimum production of all the undesired reactions.

The power consumption required to convert C_2H_4 and to produce EO as a function of the O_2/C_2H_4 feed molar ratio is shown in Figure 2d. The power consumption per EO molecule produced decreased with an increasing O_2/C_2H_4 feed molar ratio to 0.1:1 and then increased with increasing O_2/C_2H_4 feed molar ratios from 0.1:1 to 0.3:1. However, the O_2/C_2H_4 feed molar ratio only slightly affected the power consumption per

 C_2H_4 molecule converted, being in the range of 0.9–1.7 W s per C_2H_4 molecule converted. The minimum power consumption per EO molecule produced was found at a O_2/C_2H_4 feed molar ratio of 0.1:1. Hence, an O_2/C_2H_4 feed molar ratio of 0.1:1 was considered to be optimal for the maximum ethylene epoxidation performance in the DBD system when using air as the oxidant source.

3.2.2. N₂O System. N₂O was used as an oxygen source to react with C2H4 in the DBD system otherwise as per the air system (section 3.2.1).²⁴ The effect of the N₂O/C₂H₄ feed molar ratio on the ethylene epoxidation performance is shown in Figure 3. The C₂H₄ and N₂O conversion levels significantly increased as the N₂O/C₂H₄ feed molar ratio increased from 0:1 to 0.17:1 and then slightly decreased as the N_2O/C_2H_4 feed molar ratio was further increased over 0.17:1 (Figure 3a), and this was almost linear for the N2O conversion. Thus, the highest N₂O and C₂H₄ conversion levels of 42.4 and 27.4%, respectively, were obtained at a N₂O/C₂H₄ feed molar ratio of 0.17:1. It can be observed that at any given N₂O/C₂H₄ feed molar ratio, the N₂O conversion level was much higher than the C₂H₄ one, which is explained by the fact that the bond dissociation energy of N₂O (167 kJ/mol) is much lower than that of C₂H₄ (682 kJ/mol), resulting in N₂O molecules being converted more easily than C₂H₄ molecules. In addition, the plasma reaction was performed under a lean N₂O condition, leading to a higher conversion of N₂O than C₂H₄.

Interestingly, comparing between the N_2O and air systems, the N_2O conversion level was much lower than the O_2 (in air) conversion level. It is possible that the active O and N species can more easily recombine to N_2O molecules than to O_2 because the bond dissociation energy of N_2O is lower than that of O_2 . As mentioned before, the separate feed of C_2H_4 from the oxidant (C_2H_4 at the position fraction of 0.5) used in this study

Table 1. Comparison of the Parallel Plate DBD Systems on the Ethylene Epoxidation Performance

	conversion (%)					power consumption (W s/molecule)			
parallel plate DBD system (conditions)	C ₂ H ₄	O ₂	N ₂ O	EO selectivity (%)	EO yield (%)	C ₂ H ₄	EO produced		
DBD using a clear glass plate and O_2 as an oxidant ⁶²	91.0	93.7	_	6.2	5.6	0.4×10^{-16}	6.1×10^{-16}		
mixed feed, O ₂ /C ₂ H ₄ molar ratio of 1/1, gap distance of 1 cm, applied voltage of 19 kV, input frequency of 500 Hz, and total feed flow rate of 50 cm ³ /min	71.0	70.7		0.2	0.0	017 / 10	0.12 // 10		
DBD using 20 wt % Ag/SiO ₂ and O ₂ as an oxidant ²⁸	7.0	64.4	_	30.6	2.1	4.6×10^{-16}	15.3×10^{-16}		
mixed feed, O_2/C_2H_4 molar ratio of 0.25/1, gap distance of 0.7 cm, applied voltage of 19 kV, input frequency of 500 Hz, and total feed flow rate of 50 cm ³ /min									
DBD using 10 wt % Ag/glass plate and O ₂ as an oxidant ²⁹	1.6	83.0	_	72.1	1.3	23.0×10^{-16}	16.6×10^{-16}		
separate feed [C_2H_4 feed position of 0.5], O_2/C_2H_4 molar ratio of 0.2/1, gap distance of 0.7 cm, applied voltage of 19 kV, input frequency of 500 Hz, and total feed flow rate of 50 cm ³ /min									
DBD using two frosted glass plates and O ₂ as an oxidant ²⁴	19.8	99.5	_	68.1	10.9	1.9×10^{-16}	2.8×10^{-16}		
separate feed [C_2H_4 feed position of 0.5], O_2/C_2H_4 molar ratio of 0.2/1, gap distance of 0.7 cm, applied voltage of 23 kV, input frequency of 500 Hz, and total feed flow rate of 50 cm ³ /min									
DBD using two frosted glass plates and air as an oxidant (this work)	20.7	98.8	-	53.0	11.0	1.42×10^{-16}	2.74×10^{-16}		
separate feed $[C_2H_4$ feed position of 0.5], O_2 (in air)/ C_2H_4 molar ratio of 0.1/1, gap distance of 0.7 cm, applied voltage of 23 kV, input frequency of 500 Hz, and total feed flow rate of 50 cm ³ /min									
DBD using two frosted glass plates and N2O as an oxidant (this work)	27.4	_	42.4	80.1	21.9	1.27×10^{-16}	2.65×10^{-16}		
separate feed $[C_2H_4]$ feed position of 0.5], N_2O/C_2H_4 molar ratio of 0.17/1, gap distance of 0.7 cm, applied voltage of 23 kV, input frequency of 500 Hz, and total feed flow rate of 50 cm ³ /min									

caused a low residence time of C_2H_4 in the plasma reaction zone, resulting in a lower C_2H_4 conversion level compared to that for N_2O conversion. As a result, the separate feed of C_2H_4 could minimize the formation of CO and CO_2 as well as all other undesirable reactions, including the cracking, coupling, and oxidation dehydrogenation reactions.

Both the EO selectivity and yield of the N2O system exhibited a similar trend to that in the air system in that they markedly increased with increasing N2O/C2H4 feed molar ratio from 0:1 to 0.17:1 and then decreased sharply as the feed ratio increased above 0.17:1 (Figure 3b). In contrast, the CO selectivity apparently increased as the N₂O/C₂H₄ feed molar ratio increased from 0.17:1 to 0.3:1 (Figure 3c). Interestingly, this N₂O system did not produce CO₂ at any of the tested N₂O/C₂H₄ feed molar ratios, which probably reflects that the plasma system operated under a lean oxygen condition. Under the studied conditions, the main product was EO (up to 80%) followed by H₂ (about 10%) with only small amounts of CH₄, C₂H₆, C₃H₈, and CO. In addition, small amounts of tiny yellow droplets and coke were found to deposit on the glass surface, which were consistent with the small carbon loss (less than 6% from the carbon balance). The results imply that under the presence of N_2O , the ethylene epoxidation reactions (eqs 7–9) were dominant. Interestingly, the addition of N2O promoted the oxidative dehydrogenation reactions [eq 13-19], as indicated by the increase in the hydrogen selectivity from 8 to 10% when the feed molar ratio of N_2O/C_2H_2 increased from 0:1 to 0.08:1. The H₂ and CH₄ selectivities slightly increased with increasing N_2O/C_2H_4 feed molar ratios, whereas the C_2H_6 and C₃H₈ selectivities moderately decreased when the N₂O/ C₂H₄ feed molar ratio was increased from 0.08:1 to 0.3:1. In the absence of N2O (or at the lowest N2O/C2H4 feed molar ratio of 0:1), the coupling reaction for the formation of C₃H₈ (eqs 29-33) was dominant instead of the cracking reactions (eqs 24-28). The increased N₂O/C₂H₄ feed molar ratio simply increased the amount of active O species available (eqs 5 and

6) in the plasma reaction zone to initiate all the oxidation reactions (eqs 10–19) to form CO. Again, the absence of CO₂ in the product under the studied conditions can be explained by the fact that the highest N_2O/C_2H_4 feed molar ratio (0.3:1) possessed a very low oxygen concentration compared to the theoretical 6:1 ratio for the complete oxidation reaction. At the highest N_2O/C_2H_4 feed molar ratio of 0.3:1, the formation of coke spots appeared on the frosted glass plate surface (carbon loss of 3%). The formation of N_2 can be derived from the electron collision to N_2O (eq 5), ethylene epoxidation (eq 7), partial oxidation (eq 10), and oxidative dehydrogenation (eqs 13 and 16). Moreover, the presence of N_2 has previously been reported to improve the discharge stability. S5,59

Figure 3d shows the power consumption as a function of the N_2O/C_2H_4 feed molar ratio. Both the power consumption per EO molecule produced and per C_2H_4 molecule converted tended to increase steadily with increasing N_2O/C_2H_4 feed molar ratios from 0:1 to 0.3:1. Overall, a N_2O/C_2H_4 feed molar ratio of 0.17:1 was considered to be optimal for the ethylene epoxidation.

3.2.3. Comparison of the DBD Systems on Ethylene Epoxidation Performance. Table 1 shows the progression in enhancing the process performance from previous studies up to this current research. Initially, the use of 20 wt % Ag loaded on a single clear glass plate was found to increase the EO selectivity from 6.2 to 30.6% but with an even lower EO yield from 5.6 to 2.1%. Then, the use of a separate C₂H₄ feed from the oxidant (C_2H_4 injected at a feed position fraction of 0.5) increased the EO selectivity from 30.6 to 72.1% but further decreased the EO yield slightly from 2.1 to 1.3%. The use of two frosted glass plates as dielectric barrier material was found to achieve a great enhancement in the EO yield from 1.3 to 10.9% with only a slight decrease in the EO selectivity from 72.1 to 68.1%, and the discussion was given in our previous study. 24 Then, in this study, the two different oxidizing agents, air and N₂O, were investigated and compared to the use of pure

Table 2. Comparison of the Selectivities for Other Products among the Three Tested Oxidants

	selectivity (%)							
the parallel plate DBD system (conditions)	H_2	CH ₄	C_2H_6	C_3H_8	C_4H_8	C_4H_{10}	СО	CO ₂
DBD using two frosted glass plates and pure O ₂ as the oxidant ²⁴	24.8	3.9	12.0	19.2	_	_	0.5	0.6
separate feed $[C_2H_4$ feed position of 0.5], O_2/C_2H_4 molar ratio of 0.2/1, gap distance of 0.7 cm, applied voltage of 23 kV, input frequency of 500 Hz, and total feed flow rate of 50 cm ³ /min								
DBD using two frosted glass plates and air as the oxidant (this work)	10.8	2.0	3.6	1.8	_	_	0.5	_
separate feed [C_2H_4 feed position of 0.5], O_2 (in air)/ C_2H_4 molar ratio of 0.1/1, gap distance of 0.7 cm, applied voltage of 23 kV, input frequency of 500 Hz, and total feed flow rate of 50 cm ³ /min								
DBD using two frosted glass plates and N2O as the oxidant (this work)	10.3	1.9	6.0	3.6	_	_	_	_
separate feed [C_2H_4 feed position of 0.5], a N_2O/C_2H_4 molar ratio of 0.17/1, a gap distance of 0.7 cm, an applied voltage of 23 kV, an input frequency of 500 Hz, and total feed flow rate of 50 cm ³ /min								
DBD using two frosted glass plates without an oxidant (this work)	8.0	2.7	12.3	15.2	19.0	36.3	_	_
separate feed $[C_2H_4]$ feed position of 0.5], gap distance of 0.7 cm, applied voltage of 23 kV, an input frequency of 500 Hz, and total feed flow rate of 50 cm ³ /min								

O2. The use of air did not significantly change the ethylene epoxidation performance in terms of power consumption and EO selectivity and yield, but the use of N2O as the oxidant greatly enhanced both the EO selectivity and yield with only a slightly lower power consumption as compared to both the pure O_2^{24} and air (section 3.2.1) systems. The lower oxidative activity of N₂O was responsible for the enhancement of the ethylene epoxidation reaction with a lower level of all the undesirable reactions compared to both the pure O224 and air systems (Tables 1 and 2). Direct oxidation of hydrocarbon molecules, such as propane and propene, to CO_x is restrained when using $N_2O_x^{-51,60}$ That the N_2O_y system had the most superior performance of the ethylene epoxidation reaction, in terms of the highest EO selectivity and yield with lower byproducts, such as H₂, C₂H₆, and C₃H₈ selectivities without CO, CO_2 , and C_{4+} production can be explained by the fact that N₂O decomposes to N₂ and atomically mild electrophilic oxygen species, which further react with the high charge density of C=C bonds to form epoxide. 1 In addition, the generated N₂ molecules also help the discharges to become more stable. S On the other hand, the active oxygen species produced from O₂ molecules (eq 6) have a strong electrophilic character and so can effectively react with the C=C bond to favorably produce other oxygenates and CO. Hence, N2O is a more efficient free O producer, as compared to both pure O2 and air, for the ethylene epoxidation activity. However, in the absence of any oxidant, the C₂H₄ molecules collided with high energetic electrons to preferably initiate the coupling reactions (eqs 29-37) and cracking reactions (eqs 24-28), as experimentally indicated by the second and third highest product levels of C_4H_{10} and C_4H_8 , respectively (Figure 3 and Table 2).

4. CONCLUSIONS

This work comparatively studied ethylene epoxidation in the presence of the different oxidant gases (air and N_2O), in indirect comparison with pure O_2 in the same system and conditions, ²⁴ using the parallel plate DBD system with two frosted glass plates, and a separate C_2H_4 /oxidizing agent feed. The operational conditions were fixed at applied voltage of 23 kV, input frequency of 500 Hz, C_2H_4 feed position fraction of 0.5, and total feed flow rate of 50 cm³/min (residence time of 0.81 min) to maintain similar plasma behaviors to the previously reported work with pure O_2 . Of the different oxidant systems, the N_2O system exhibited a superior performance in terms of the highest EO selectivity (80.1%) and EO yield (21.9%) with lowest power consumption.

Attractively, the EO yield from the DBD system in the presence of N_2O was 2-fold higher than that in the O_2 system. The use of N_2O can reduce all the undesirable reactions, including the oxidative dehydrogenation, cracking, and CO formation reactions. The coupling reactions to form C_4H_{10} and C_4H_8 were dominant in the absence of any oxidants. Further research should investigate the combination of this DBD system with supported Ag catalysts in order to further enhance the EO selectivity and yield.

AUTHOR INFORMATION

Corresponding Author

*Tel.: +66-2-218-4139. Fax: +66-2-218-4139. E-mail: sumaeth. c@chula.ac.th.

ORCID ®

Sumaeth Chavadej: 0000-0001-6790-8521

Notes

The authors declare no competing financial interest.

ACKNOWLEDGMENTS

This research was supported by King Mongkut's University of Technology North Bangkok (KMUTNB 60-ART-011) and Thailand Research Fund (Grant MRG5980154) to T.S. and the TRF Senior Research Scholar Grant (RTA578008) to S.C. The Center of Excellence on the Petrochemical and Materials Technology, Chulalongkorn University, is also acknowledged for providing partial funding for this project.

REFERENCES

- (1) Lefort, T. French Patent 729952, 1931.
- (2) Hassani, S. S.; Ghasemi, M. R.; Rashidzadeh, M.; Sobat, Z. Nanosized silver crystals and their dispersion over α -alumina for ethylene epoxidation. *Cryst. Res. Technol.* **2009**, 44 (9), 948–952.
- (3) McClellan, P. P. Manufacture and Uses of Ethylene Oxide and Ethylene Glycol. *Ind. Eng. Chem.* **1950**, 42 (12), 2402–2407.
- (4) Amorim de Carvalho, M. C. N.; Passos, F. B.; Schmal, M. Study of the active phase of silver catalysts for ethylene epoxidation. *J. Catal.* **2007**, 248 (1), 124–129.
- (5) Özbek, M. O.; Van Santen, R. A. The mechanism of ethylene epoxidation catalysis. *Catal. Lett.* **2013**, *143* (2), 131–141.
- (6) Dellamorte, J. C.; Lauterbach, J.; Barteau, M. A. Palladium—silver bimetallic catalysts with improved activity and selectivity for ethylene epoxidation. *Appl. Catal., A* **2011**, *391* (1–2), 281–288.
- (7) Diao, W.; DiGiulio, C. D.; Schaal, M. T.; Ma, S.; Monnier, J. R. An investigation on the role of Re as a promoter in $AgCsRe/\alpha$ - Al_2O_3 high-selectivity, ethylene epoxidation catalysts. *J. Catal.* **2015**, 322 (0), 14–23.

- (8) Jankowiak, J. T.; Barteau, M. A. Ethylene epoxidation over silver and copper-silver bimetallic catalysts: II. Cs and Cl promotion. *J. Catal.* **2005**, 236 (2), 379–386.
- (9) Dellamorte, J. C.; Lauterbach, J.; Barteau, M. A. Rhenium promotion of Ag and Cu-Ag bimetallic catalysts for ethylene epoxidation. *Catal. Today* **2007**, *120* (2), 182–185.
- (10) Piccinin, S.; Stampfl, C.; Scheffler, M. First-principles investigation of Ag-Cu alloy surfaces in an oxidizing environment. *Phys. Rev. B: Condens. Matter Mater. Phys.* **2008**, *77*, 7.
- (11) Torres, D.; Lopez, N.; Illas, F. A theoretical study of coverage effects for ethylene epoxidation on Cu (111) under low oxygen pressure. *J. Catal.* **2006**, 243 (2), 404–409.
- (12) Goncharova, S. N.; Paukshtis, E. A.; Bal'zhinimaev, B. S. Size effects in ethylene oxidation on silver catalysts. Influence of support and Cs promoter. *Appl. Catal., A* 1995, 126 (1), 67–84.
- (13) Eliasson, B.; Kogelschatz, U. Nonequilibrium volume plasma chemical processing. *IEEE Trans. Plasma Sci.* **1991**, 19 (6), 1063–1077.
- (14) Fridman, A.; Gutsol, A.; Cho, Y. I. Non-thermal atmospheric pressure plasma. In *Advances in Heat Transfer*, 2007; Vol. 40, pp 1–14210.1016/S0065-2717(07)40001-6.
- (15) Zheng, X.; Tan, S.; Dong, L.; Li, S.; Chen, H. LaNi O_3 @Si O_2 core-shell nano-particles for the dry reforming of CH₄ in the dielectric barrier discharge plasma. *Int. J. Hydrogen Energy* **2014**, 39 (22), 11360—11367.
- (16) Jo, S.; Kim, T.; Lee, D. H.; Kang, W. S.; Song, Y.-H. Effect of the Electric Conductivity of a Catalyst on Methane Activation in a Dielectric Barrier Discharge Reactor. *Plasma Chem. Plasma Process.* **2014**, 34 (1), 175–186.
- (17) Jin, L.; Li, Y.; Lin, P.; Hu, H. CO_2 reforming of methane on Ni/ γ -Al₂ O_3 catalyst prepared by dielectric barrier discharge hydrogen plasma. *Int. J. Hydrogen Energy* **2014**, *39* (11), 5756–5763.
- (18) Li, Y.; Xu, G.-h.; Liu, C.-j.; Eliasson, B.; Xue, B.-z. Co-generation of Syngas and Higher Hydrocarbons from CO₂ and CH₄ Using Dielectric-Barrier Discharge: Effect of Electrode Materials. *Energy Fuels* **2001**, *15* (2), 299–302.
- (19) Zhang, Y.-p.; Li, Y.; Wang, Y.; Liu, C.-j.; Eliasson, B. Plasma methane conversion in the presence of carbon dioxide using dielectric-barrier discharges. *Fuel Process. Technol.* **2003**, 83 (1–3), 101–109.
- (20) Goujard, V.; Tatibouët, J.-M.; Batiot-Dupeyrat, C. Use of a non-thermal plasma for the production of synthesis gas from biogas. *Appl. Catal., A* **2009**, 353 (2), 228–235.
- (21) Wang, Q.; Yan, B.-H.; Jin, Y.; Cheng, Y. Investigation of Dry Reforming of Methane in a Dielectric Barrier Discharge Reactor. *Plasma Chem. Plasma Process.* **2009**, 29 (3), 217–228.
- (22) Chung, W.-C.; Pan, K.-L.; Lee, H.-M.; Chang, M.-B. Dry Reforming of Methane with Dielectric Barrier Discharge and Ferroelectric Packed-Bed Reactors. *Energy Fuels* **2014**, 28 (12), 7621–7631.
- (23) Liu, S. Y.; Mei, D. H.; Shen, Z.; Tu, X. Nonoxidative Conversion of Methane in a Dielectric Barrier Discharge Reactor: Prediction of Reaction Performance Based on Neural Network Model. *J. Phys. Chem.* C **2014**, *118* (20), 10686–10693.
- (24) Chavadej, S.; Dulyalaksananon, W.; Suttikul, T. Ethylene epoxidation in a low-temperature parallel plate dielectric barrier discharge system with two frosted glass plates. *Chem. Eng. Process.* **2016**, *107*, 127–137.
- (25) Sreethawong, T.; Permsin, N.; Suttikul, T.; Chavadej, S. Ethylene epoxidation in low-temperature AC dielectric barrier discharge: Effect of electrode geometry. *Plasma Chem. Plasma Process.* **2010**, 30 (4), 503–524.
- (26) Suttikul, T.; Kodama, S.; Sekiguchi, H.; Chavadej, S. Ethylene epoxidation in an AC dielectric barrier discharge jet system. *Plasma Chem. Plasma Process.* **2014**, *34* (1), 187–205.
- (27) Suttikul, T.; Tongurai, C.; Sekiguchi, H.; Chavadej, S. Ethylene epoxidation in cylindrical dielectric barrier discharge: Effects of separate ethylene/oxygen feed. *Plasma Chem. Plasma Process.* **2012**, 32 (6), 1169–1188.

- (28) Suttikul, T.; Sreethawong, T.; Sekiguchi, H.; Chavadej, S. Ethylene epoxidation over alumina- and silica-supported silver catalysts in low-temperature AC dielectric barrier discharge. *Plasma Chem. Plasma Process.* **2011**, *31* (2), 273–290.
- (29) Suttikul, T.; Paosombat, B.; Santikunaporn, M.; Leethochawalit, M.; Chavadej, S. Improvement of ethylene epoxidation in a parallel plate dielectric barrier discharge system by ethylene/oxygen separate feed and Ag catalyst. *Ind. Eng. Chem. Res.* **2014**, *53* (10), 3778–3786.
- (30) Kogelschatz, U.; Eliasson, B.; Egli, W. From ozone generators to flat television screens: history and future potential of dielectric-barrier discharges. *Pure Appl. Chem.* **1999**, *71* (10), 1819–1828.
- (31) Ono, R.; Oda, T. Ozone production process in pulsed positive dielectric barrier discharge. J. Phys. D: Appl. Phys. 2007, 40 (1), 176.
- (32) Yuan, D.; Wang, Z.; Ding, C.; He, Y.; Whiddon, R.; Cen, K. Ozone production in parallel multichannel dielectric barrier discharge from oxygen and air: the influence of gas pressure. *J. Phys. D: Appl. Phys.* **2016**, 49 (45), 455203.
- (33) Redolfi, M.; Makhloufi, C.; Ognier, S.; Cavadias, S. Oxidation of kerosene components in a soil matrix by a dielectric barrier discharge reactor. *Process Saf. Environ. Prot.* **2010**, *88* (3), 207–212.
- (34) Aggelopoulos, C. A.; Tsakiroglou, C. D.; Ognier, S.; Cavadias, S. Non-aqueous phase liquid-contaminated soil remediation by ex situ dielectric barrier discharge plasma. *Int. J. Environ. Sci. Technol.* **2015**, *12* (3), 1011–1020.
- (35) Aggelopoulos, C. A.; Svarnas, P.; Klapa, M. I.; Tsakiroglou, C. D. Dielectric barrier discharge plasma used as a means for the remediation of soils contaminated by non-aqueous phase liquids. *Chem. Eng. J.* **2015**, *270*, 428–436.
- (36) Li, X.; Zhang, H.; Luo, Y.; Teng, Y. Remediation of soil heavily polluted with polychlorinated biphenyls using a low-temperature plasma technique. *Front. Environ. Sci. Eng.* **2014**, *8* (2), 277–283.
- (37) Lu, N.; Lou, J.; Wang, C. H.; Li, J.; Wu, Y. Evaluating the Effects of Silent Discharge Plasma on Remediation of Acid Scarlet GR-Contaminated Soil. *Water, Air, Soil Pollut.* **2014**, 225 (6), 1991.
- (38) Sun, M. Y.; Jo, J.-O.; Lee, H.-J. Dielectric Barrier Discharge Plasma-Induced Photocatalysis and Ozonation for the Treatment of Wastewater. *Plasma Sci. Technol.* **2008**, *10* (1), 100.
- (39) Duan, L.; Shang, K.; Lu, N.; Li, J.; Wu, Y. Study on the factors influencing phenol degradation in water by dielectric barrier discharge (DBD). *J. Phys.: Conf. Ser.* **2013**, *418* (1), 012129.
- (40) Kostov, K. G.; Hamia, Y. A. A.; Mota, R. P.; dos Santos, A. L. R.; Nascente, P. A. P. Treatment of polycarbonate by dielectric barrier discharge (DBD) at atmospheric pressure. *J. Phys.: Conf. Ser.* **2014**, *511* (1), 012075.
- (41) Dumitrascu, N.; Topala, I.; Popa, G. Dielectric barrier discharge technique in improving the wettability and adhesion properties of polymer surfaces. *IEEE Trans. Plasma Sci.* **2005**, 33 (5), 1710–1714.
- (42) Kostov, K. G.; Santos, A. L. R. d.; Nascente, P. A. P.; Kayama, M. E.; Mota, R. P. Modification of polyethylene terephthalate by atmospheric pressure dielectric barrier discharge (DBD) in view of improving the polymer wetting properties. *Journal of Physics: Conference Series* **2012**, 356 (1), 012006.
- (43) Zhi, F.; Jinguo, L.; Hao, Y.; Yuchang, Q.; Kuffel, E. Polyethylene Terephthalate Surface Modification by Filamentary and Homogeneous Dielectric Barrier Discharges in Air. *IEEE Trans. Plasma Sci.* **2009**, *37* (5), 659–667.
- (44) Beyer, E. M. Effect of Silver Ion, Carbon Dioxide, and Oxygen on Ethylene Action and Metabolism. *Plant Physiol.* **1979**, *63* (1), 169–173.
- (45) Suttikul, T.; Yaowapong-aree, S.; Sekiguchi, H.; Chavadej, S.; Chavadej, J. Improvement of ethylene epoxidation in low-temperature corona discharge by separate ethylene/oxygen feed. *Chem. Eng. Process.* **2013**, *70*, 222–232.
- (46) Severin, K. Synthetic chemistry with nitrous oxide. *Chem. Soc. Rev.* **2015**, 44 (17), 6375–6386.
- (47) Parmon, V. N.; Panov, G. I.; Uriarte, A.; Noskov, A. S. Nitrous oxide in oxidation chemistry and catalysis: application and production. *Catal. Today* **2005**, *100* (1–2), 115–131.

- (48) Voskresenskaya, E. N.; Kurteeva, L. I.; Pervyshina, G. G.; Anshits, A. G. Comparison of O_2 and N_2O as oxidants for the oxidative coupling of methane over Bi-containing oxide catalysts. *Catal. Today* **1995**, 24 (3), 277–279.
- (49) Sobolev, V. I.; Koltunov, K. Y. Gas-phase Oxidation of Alcohols with O_2 and N_2O Catalyzed by Au/Ti O_2 : A Comparative Study. *Catal. Lett.* **2015**, 145 (2), 583–588.
- (50) Hoelderich, W. F.; Kollmer, F. Oxidation reactions in the synthesis of fine and intermediate chemicals using environmentally benign oxidants and the right reactor system. *Pure Appl. Chem.* **2000**, 72, 1273.
- (51) Held, A.; Kowalska-Kuś, J.; Nowińska, K. Propane-to-propene oxide oxidation on silica-supported vanadium catalysts with N_2O as an oxidant. *J. Catal.* **2016**, 336, 23–32.
- (52) Held, A.; Kowalska-Kuś, J.; Łapiński, A.; Nowińska, K. Vanadium species supported on inorganic oxides as catalysts for propene epoxidation in the presence of N_2O as an oxidant. *J. Catal.* **2013**, 306 (0), 1–10.
- (53) Chavadej, S.; Kiatubolpaiboon, W.; Rangsunvigit, P.; Sreethawong, T. A combined multistage corona discharge and catalytic system for gaseous benzene removal. *J. Mol. Catal. A: Chem.* **2007**, 263 (1–2), 128–136.
- (54) Marchalant, P. J.; Whelan, C. T.; Walters, H. R. J. Excitation—Ionization and Excitation—Autoionization of Helium. In *Coincidence Studies of Electron and Photon Impact Ionization*; Whelan, C. T., Walters, H. R. J., Eds.; Springer: Boston, MA, 1997; pp 21–43.
- (55) Fletcher, J. D.; Parkes, M. A.; Price, S. D. Bond-forming reactions of N₂2+ with C₂H₄, C₂H₆, C₃H₄ and C₃H₆. *Int. J. Mass Spectrom.* **2015**, 377, 101–108.
- (56) Lau, W. S.; Qian, P. W.; Han, T.; Sandler, N. P.; Che, S. T.; Ang, S. E.; Tung, C. H.; Sheng, T. T. Evidence that N_2O is a stronger oxidizing agent than O_2 for both Ta_2O_5 and bare Si below 1000 °C and temperature for minimum low-K interfacial oxide for high-K dielectric on Si. *Microelectron. Reliab.* **2007**, 47 (2–3), 429–433.
- (57) Tao, X.; Bai, M.; Li, X.; Long, H.; Shang, S.; Yin, Y.; Dai, X. CH₄–CO₂ reforming by plasma challenges and opportunities. *Prog. Energy Combust. Sci.* **2011**, *37* (2), 113–124.
- (58) Indarto, A.; Choi, J.-W.; Lee, H.; Song, H. K. Effect of additive gases on methane conversion using gliding arc discharge. *Energy* **2006**, *31* (14), 2986–2995.
- (59) Long, H.; Shang, S.; Tao, X.; Yin, Y.; Dai, X. CO2 reforming of CH4 by combination of cold plasma jet and Ni/ γ -Al₂O₃ catalyst. *Int. J. Hydrogen Energy* **2008**, 33 (20), 5510–5515.
- (60) Woods, M. P.; Mirkelamoglu, B.; Ozkan, U. S. Oxygen and Nitrous Oxide as Oxidants: Implications for Ethane Oxidative Dehydrogenation over Silica—Titania-Supported Molybdenum. *J. Phys. Chem. C* 2009, 113 (23), 10112—10119.
- (61) Sun, C. X.; Wang, Y.; Jia, A. P.; Chen, S. X.; Luo, M. F.; Lu, J. Q. Gas-phase epoxidation of 3,3,3-trifluoropropylene over Au/CuTiO₂ catalysts with N₂O as the oxidant. *J. Catal.* **2014**, *312*, 139–151.
- (62) Sreethawong, T.; Suwannabart, T.; Chavadej, S. Ethylene epoxidation in low-temperature AC dielectric barrier discharge: Effects of oxygen-to-ethylene feed molar ratio and operating parameters. *Plasma Chem. Plasma Process.* **2008**, 28 (5), 629–642.